INVESTIGATION OF METEOROLOGICAL CONDITION DURING AIR DYNASTY HELICOPTER CRASH USING WRF MODEL

A Dissertation Submitted to

Central Department of Hydrology and Meteorology, Tribhuvan University

Kirtipur, Kathmandu

In a partial fulfillment of the requirements for the Degree of Master of Science (M.Sc.) in Hydrology and Meteorology awarded by Tribhuvan University, Kirtipur , Kathmandu, Nepal

By

Saroj Pudasainee

Symbol No: 209/075

T.U. Regd. No.:5-2-37-867-2014

August, 2022

DECLARATION

I, hereby, declare that this project entitled **"Investigation of meteorological condition during Air Dynasty Helicopter crash using WRF model"** is my own genuine work and has not been submitted anywhere for the award of any degree. All sources of information have been duly acknowledged.

.....

Saroj Pudasainee

August, 2022 A.D

LETTER OF RECOMMENDATION

This is to recommend that the dissertation entitled **"Investigation of meteorological condition during the Air Dynasty Helicopter crash using the WRF model"** has been carried out by Mr. Saroj Pudasainee for the partial fulfillment of a Master's Degree in Science in Hydrology and Meteorology. This is the original work and has been carried out under my supervision. To the best of my knowledge, this thesis work has not been submitted for any other degree at any institution.

Therefore, I recommend this dissertation for approval and acceptance.

…….

Supervisor

Dr. Binod Dawadi

Associate Professor

Central Department of Hydrology and Meteorology

Tribhuvan University

Kirtipur, Kathmandu

CERTIFICATION

This dissertation entitled **"Investigation of meteorological condition during Air Dynasty Helicopter crash using WRF model""** which is submitted to Central Department of Hydrology and Meteorology for the partial fulfillment of degree of Masters of Science (M.Sc.) is research work carried out by me under supervision of Dr. Binod Dawadi, Central Department of Hydrology and Meteorology, Kirtipur, Kathmandu. This research is my own genuine work and has not been submitted anywhere for the award of any degree.

APPROVED BY:

……
Signature
Supervisor
Dr. Binod Dawadi
Associate Professor
CDHM
Tribhuvan University
Kirtipur, Kathmandu, Nepal

……
Signature
External examiner
Dr. Indira Kandel
Senior Division Meteorologist
DHM
Kathmandu, Nepal

……
Signature
Co-supervisor
Dr. Dibas Shrestha
Assistant Professor
CDHM
Tribhuvan University
Kirtipur, Kathmandu, Nepal

……
Signature
Internal examiner
Dr. Binod Pokharel
Associate Professor
CDHM
Tribhuvan University
Kirtipur, Kathmandu, Nepal

……
Signature
Co-supervisor
Mr. Netra Jit Khadka
CDHM
Tribhuvan University
Kirtipur, Kathmandu, Nepal

……
Signature
Head of Department
Prof. Dr. Deepak Aryal
CDHM
Tribhuvan University
Kirtipur, Kathmandu, Nepal

ACKNOWLADGEMENT

First and foremost I offer my sincerest gratitude to my research work supervisor Dr. Binod Dawadi, Associate Professor of Central Department of Hydrology and Meteorology, Kirtipur, Kathmandu. Who has supported me throughout the research work with his guidance, encouragement and effort in conducting this thesis without him this project work would not have been completed.

I am extremely grateful and would like to offer warm gratitude to my co-supervisors Dr. Dibas Shrestha, Assistant Professor, and Mr. Netra Jit Khadka, Central Department of Hydrology and Meteorology, Kirtipur, Kathmandu for supporting me with their patience, knowledge, and endless encouragement during the course of this thesis and without their endless help this thesis would be incomplete. I am also very grateful to our head of department Prof. Dr. Deepak Aryal for providing opportunity, for understanding and continuous support in every situation.

I am also very thankful to Mr. Ram Hari Aacharya, Assistant Professor, Department of Tri- Chandra Campus, Ghantaghar Kathmandu and Mr. Jeevan Bhandari for his help, motivation, encouragement, ideas for analysis from the beginning of the study. I would like to thank Mr. Kumar Rana for his help in different time intervals. I am thankful to each and every respected teachers and staff of Central Department of Hydrology and Meteorology, Kathmandu, Nepal for encouragement and help throughout the study.

I would like to thank the Research Directorate, Rector's Office T.U. Kirtipur for providing the Dissertation Grant awarded to conduct this research. I am also grateful to my family for their continuous support from the beginning of the study. I would like to share my success with everyone who are related with it directly or indirectly.

Saroj Pudasainee

August, 2022 A.D

ABSTRACT

Mountain flight remains a considerable challenge in Nepal because of rugged terrain. Since 1979 A.D, there have been 36 helicopter accidents over different parts of the country that have claimed 85 lives. Most of the accidents are reported to have unfavorable weather conditions as the main cause. However, the detailed meteorological analysis for most of the accidents has not been done yet. A detailed understanding of the meteorological condition and reliable forecast that may developed over the complex terrain of the mid-hills of Eastern Nepal Himalaya is yet to be achieved. This study assesses the weather conditions possibly associated with the most recent fatal crash at Pathivara Peak on 27 February 2019 using Advanced Research version of the Weather Research and Forecasting (WRF-ARW) model. Prevailing weather condition during accident time such as; low ceiling with cloud base, light to moderate snowfall, poor visibility, below freezing temperature, high amount of water droplets suggests possible icing on rotor. Icing could be major factor responsible for the fatal crash. WRF-ARW was reasonably able to simulate the weather condition. This research recommended that aviation stakeholders and pilots should fly only after a clear route forecast over the complex geographical condition for the safety of flights.

Keywords: Aviation, Forecast, Icing, Visibility, WRF-ARW

Table of Contents

List of Figure

List of Tables

List of Abbreviations

ADH	Air Dynasty Helicopter
AMSL	Meters Above Mean Sea Level
ANS	Air Navigation System
ARW	Advanced Research Weather Research and Forecasting
AWS	Automatic Weather Station
CAAN	Civil Aviation Authority of Nepal
CDHM	Central Department of Hydrology and Meteorology
CFIT	Controlled Flight into Terrain
dBZ	Decibel Relative to Z
EDT	Eastern Daylight Time
DHM	Department of Hydrology and Meteorology
GFS	Global Forecasting System
hPa	Hectopascal
IMC	Instrumental Meteorological Condition
INSAT	Indian Satellite
L.FR	Lewis Fry Richardson
LST	Land Surface Temperature
LTO	Landing and Take Off
MYJ	Mellor Yamada Janjic
NCEP	National Centre Environment Programme
NWP	Numerical Weather Prediction
PBL	Planetary Boundary Layer
PC	Picture Credit
PIC	Pilot in Command
RADAR	Radio Detection and Ranging
RH	Relative Humidity
RRTM	Rapid Radiative Transfer Model
SLD	Super Cooled Liquid Droplets

TIA	Tribhuvan International Airport
UTC	Universal Co-ordinated Time
USGS	United States Geological Survey
VHF	Very High Frequency
VIP	Very Important Person
VRF	Visual Flight Rules
VNKT	Tribhuvan International Airport
WD	Western Disturbance
WMO	World Meteorological Organization
WPS	WRF Preprocessing System
WRF	Weather Research and Forecasting Model

CHAPTER-I

INTRODUCTION

1.1 Background

With a boom in the tourism sector in Nepal, middle-class tourists from different countries have started roughly flying over the Himalayan terrain over the last decade. This influx of tourists stretches its aviation sector, in a country with some of the most vulnerable airports. The complex topography over middle mountain creates atmospheric instability and hazardous meteorological condition to the Aviation safety. (Regmi, Kitada, & Kurata, 2003). An aircraft is most vulnerable to ground impact and few seconds are available to a pilot to recover lost control during landing and Take-off (LTO). During the late afternoon and evening, the valley walls cool quickly, cooling a layer of air next to the slope. This denser air moves downslope into the valley causing the mountain breeze (gravity or drainage wind). The slopes cool at a rate faster than they heat up, so the mountain breeze may be stronger than the valley breeze, averaging 10-12 knots. Winds associated with mountainous terrain are generally of two types. Terrain-forced flows are produced when large-scale winds are modified or channeled by the underlying complex terrain. Diurnal mountain winds are produced by temperature contrasts that form within the mountains or between the mountains and the surrounding plains and are therefore also called Thermally Driven Circulations. (Whiteman, 2000)

Indeed, Nepal has been the location of a series of aircraft accidents. Since the first aircraft accident on 7 May 1946, there have been 32 fatal accidents, with 701 casualties and numerous other minor accidents. These frequent aircraft accidents have raised serious concerns about civil aviation and the safety of passengers. However, necessary thought and serious research on aviation weather hazards are yet to be seen in the country. This research-based on the Air Dynasty Helicopter (ADH) crash on 27 February 2019 at Sisne Khola in Taplejung district killing the seven people on board. The investigation team also reported that ADH crashed due to unfavorable weather conditions while takeoff from the Pathivara Temple.

The role of airlines in the total tourism business is to provide mass and quick transportation between countries under safe, standardized, and economic conditions. Its

relationship to the tourism industry is better understood by breaking down the entire activity of tourism into its parts. Because of quick and efficient transportation, people are spurred to travel for various reasons as destinations have become more accessible.

1.2 General Information of accidents

An Airbus helicopter H15 (AS350B3e), 9N-AMI, owned and operated by Air Dynasty Heli Pvt. Ltd, Nepal carrying 7 Nepalese passengers along with the Captain, crashed on date February 27 2019 at Sisne Khola, Taplegung district, Province No 1 with-in a minute after takeoff from Pathivara towards Tribhuvan International Airport (TIA), Kathmandu with casualties of all onboard the helicopter including the Minister of Culture, Tourism and Civil Aviation.

The VIP flight was approved to fly on the VNKT-Panchthar-VNKT sector by the TIA office on February 27, 2019. Even though the approved flight plan was for Panchthar with ETD of 0230 UTC, the PIC requested the tower to change the destination to Terathum in VHF indicating VIP on board. The flight was then approved for the VNKT-Terathum-VNKT sector. The helicopter departed from VNKT at 0246 UTC (08:31 LST) and arrived at Terathum at 0409 UTC (9:54 LST). As per the scheduled plan, the helicopter was supposed to fly back to VNKT from Terathum but the helicopter departed from Chuhandada Terathum at 0545 UTC (11:30LT) and proceeded to Pathibhara without prior approval and landed at approximately 0604 UTC (11:49 LST). Around forty-five minutes later, at 0649 UTC (12:34 LT), the helicopter departed for VNKT and met with a fatal accident within a minute later. The aircraft crashed at an altitude of 10350 ft. coordinated at $N27^{0}25'42''$, $E087^{0}45'59''$. The crash site was about 5.49NM NNE from Taplegung airport and the helicopter was found destroyed due to an impact on a rocky hill followed by post-crash fire. (Figure 1)

The helicopter was flying under visual flight rules (VFR) in instrumental meteorological conditions. After departure from Pathivara at an elevation of 12427 feet, the MSL helicopter took off on a north-westerly heading and started to turn then continued turning high-speed speed descent at the rate of about 3600 feet per minute and impacted at a distance of 0.02 NM west from Pathivara helipad at an elevation of 10,350 feet. The accident investigation commission report (Helicopter Accident Investigation Commission 2020) concluded that the probable cause of the accident was the PIC, who was possibly affected with euphoria (initial phase of hypoxia)

immediately after take-off from the Pathibhara helipad in unfavorable weather and encountered strong gusting wind along with snowfall which led him to inadvertently enter into IMC conditions, ended with the tragic crash. Condensation inside the windshield and icing on the outside of the windshield reduced outside visibility.

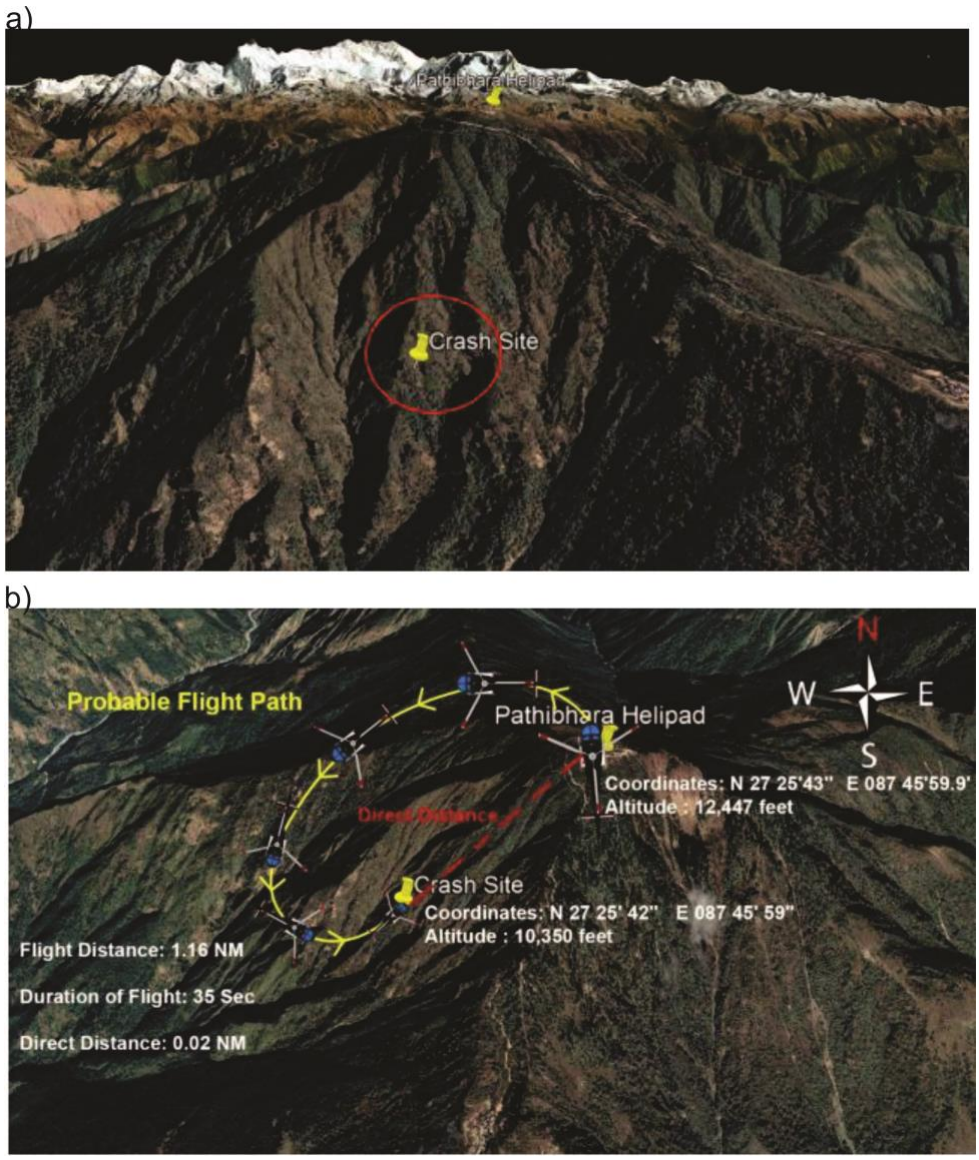

Figure 1: (a) Crash event site and (b) Flight path of Air Dynasty over complex terrain plotted on Google Earth image Source: Helicopter accident investigation commission, 2020

1.3 Rationale

Changing Weather patterns over the place is hazardous for Aircraft and Air Navigation systems (ANS). According to World Meteorological Organization (WMO), most aircraft over the complex terrain happened due to orographically induced turbulence. Strong downslope wind (Drainage Wind) flowing around the edge of the mountain might be a destructing factor for the Aircraft (Whiteman, 2000). Mountain waves and

hydraulic jumps over the slope of the Mountain are hazardous for low-level aviation, particularly for low-level aircraft (Regmi & Maharjan, 2015).

Also, this research will be able to identify the possible meteorological condition during the time of the accident. It will help to simulate the weather hazards that occur over an accident site is carried out using Weather Research and Forecasting (WRF) Model.

The event happened very recently with VIP was lost their life during the crash. Some research suggests that such types of multiple accidents happened every year and most of them are blamed to unfavorable weather condition and weakness of pilot. But, details studies using available ground based data and model simulation are still rare. This study will help to find the technique of routine forecast over the different parts of the country that is useful for the flight navigation system, which is very useful for the tourism sector too. Also, this research will give a positive message for the tourist as Nepal is meteorologically safe for visiting.

1.4 Research question

Research questions are formulated to visualize the curiosity after the literature review which is listed below.

1. Is WRF model able to forecast weather over a region?
2. What could be the possible meteorological condition during the time of the accident?
3. What could be the driving weather factors for this helicopter crash?

1.5 Objective of Study

The main motto of this research work is to investigate the possible meteorological conditions during the incident using the WRF modeling system.

The main objectives of the study are:

1. To identify the possible low-level meteorological conditions during the time of the accident.
2. Simulate the prevalent weather hazards around an accident site using WRF model.
3. To identify the most probable weather factors associated to the accident.

CHAPTER-II

LITERATURE REVIEW

2.1 Background

The deposition of atmospheric moisture on the land surface is commonly known as precipitation. This moisture falls on the earth's surface in several forms like rainfall, sheet, virga, snowfall, hail, and so on. The presence of low-level convective clouds that forms this type of unstable weather condition is hazardous for the Aircraft. The complex terrain of Nepal Himalaya creates unstable meteorological conditions and forms its own mesoscale systems. These mesoscale flows may trigger highly localized extreme weather (Regmi et al., 2003; Regmi & Maharjan, 2015). Unpredictable weather patterns together with the extreme topographic complexities of the region often pose unprecedented risks for aviation activities in Nepal. Mostly Nepalese airports are located in the deep valley, terrian side, river gorge, or southern slope of mountains. Air routes connecting these airports cross numerous high mountain ridges, pass through mountain gaps, and often plunge deep into and follow innumerable narrow winding river gorges (Regmi, 2015b). The user of the WRF Model to simulate atmospheric processes over complex mountainous terrain has been rigorously tested around the world (Jiménez et al., 2013; P. Kumar et al., 2015; Lee et al., 2015) including Nepal Himalaya. A few examples of WRF modeling over the Himalaya region were in studies of precipitation patterns over the greater Himalaya (Maussion et al., 2014), the large-scale interaction between topography and precipitation (Bookhagen and Burbank 2006), atmosphere–glacier feedback (Collier & Immerzeel, 2015), extreme snowfall (Norris et al., 2015), aviation weather hazards over one of the world's most extreme airports, the Jom-som Airport (Regmi, 2015a). The WFR model simulation investigated the severe turbulence at an altitude of 11.2km from the mean sea level (MSL) (Kim & Chun, 2012 et.al), generated by strong vertical wind shear associated (Sharman et al., 2012) with dissipating deep convection. (Sharman et al., 2012) found that a Clear Air Turbulence (CAT) encounter incident of a commercial aircraft at 10-km elevation was due to mountain-wave turbulence by analyzing both digital flight data recorder (DFDR)

Table 1: Record of Helicopter accident in Nepal focus on people on board

SN	Date	Operate/Type	Fatalities/ People on board	Place
1	27 Feb 2019	Air Dynasty(AS 350 B3 E ,9N-AMI)	7/7	Pathivara/Taplejung
2	8 Sept 2018	Altitude Air (AS 350 B3, 9N-ALS)	6/7	Dhading
3	14 Aug 2018	Manang Air (AS 350 B)	1/7	Hilsa, Humla
4	08 Aug 2016	Fishtail Air (AS 350B3, 9N-AKA)	7/7	Betani , Nuwakot
5	02 Jun 2015	Mountain Helicopter (AS350B3,9N)	4/4	Sindhupalchok
6	03 Aug 2014	Fishtail Air (AS 350B3, 9N-AJI)	1/1	Sindhupalchok
7	19 Jun 2013	Fishtail Air (AS 350B3, I-VIEW)	1/6	Simikot, Muchu
8	07 Nov 2010	Fishtail Air (AS 350B3, 9N-AIX)	2/2	AmadablamMountain
9	23 Sept 2006	Shree Airlines (MI-17, 9N-AHJ)	24/24	Ghunsa, Taplejung
10	04 Jan 2005	Air Dynasty Heli Services	3/3	Thhose ,Ramechhap
11	28 May 2003	Simrik Air (MI-17 IV, 9N-ADP)	2/8	Everest Base Camp
12	30 Sept 2002	Asian Airlines (MI-17, 9N-ACU)	11/11	Sholukhumbu
13	12 Nov 2001	Fishtail Air (AS-350B, 9NAFP)	4/6	Rara Lake, Mugu
14	24 Oct 1998	Asian Airlines (AS-350B, 9N-ACY)	3/3	MulKhark
15	30 Sept 1997	Karnali Air (AS-350, 9N-AEC)	1/5	ThuptenCholing
16	27 Dec 1979	VVIP (Allutte-III, 9N-RAE)	6/6	Langtang

Source: https://caanepal.gov.np/publication/aviation-safety-report/2020

Figure 2 shows the domestic flight routes within Nepal. There are 40 domestic airports in Nepal. Most of the airports are situated in complex geographical terrain where the virtual function of weather occurred. It is very challenging for meteorologists to identify the weather over such a region. For such a case, the WRF model was used to find the weather over regions as a Numerical Weather Prediction (NWP).

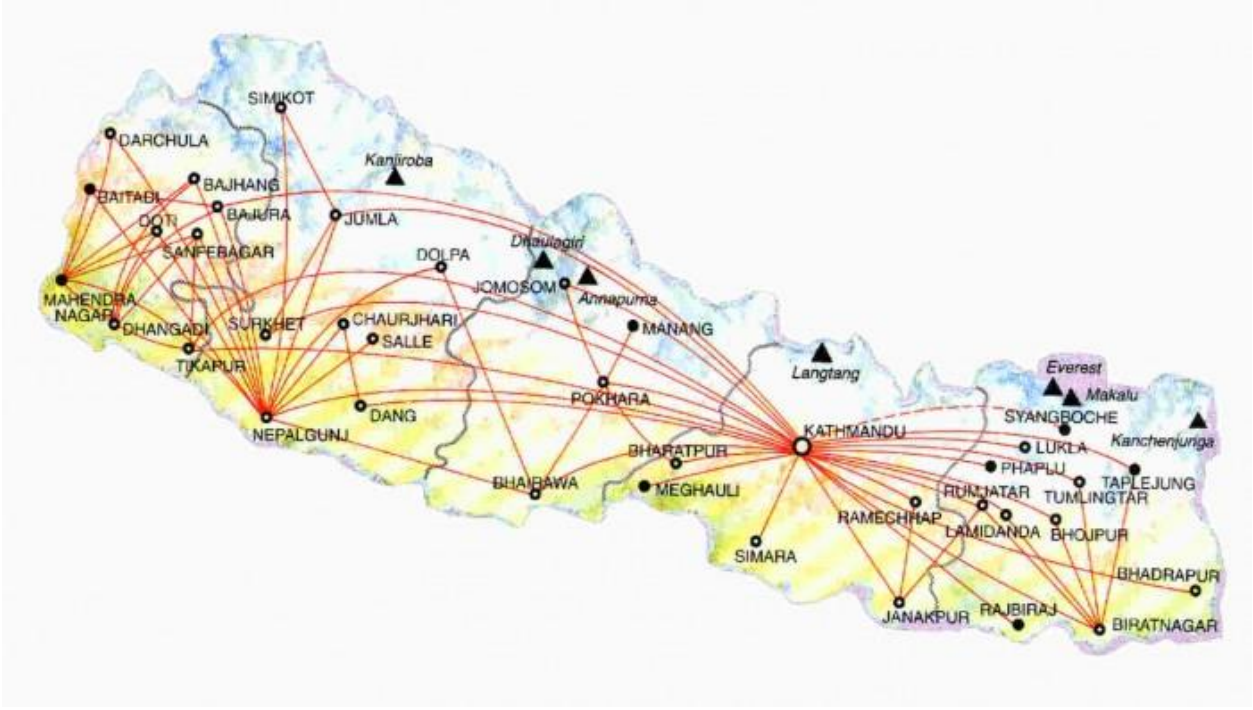

Figure 2: Flight routes within Nepal (Source: nepalflightticketbooking.com 2022)

`

2.2 Numerical Weather Prediction

Numerical prediction is a highly specialized field, which is continually involved. Operational forecast centers utilize complex prediction models that require the largest available supercomputers to obtain a solution. The British scientist L.F Richardson made the first attempt to predict the weather numerically. The differential equations governing atmospheric motions could be written approximately as a set of algebraic equations for values of the tendencies of various field variables at a finite number of points in space. (Holton, 1973)

Extreme weather events such as tornadoes, thunderstorms, hailstorms, cyclones, floods, landslides, thunderbolts, and so on happen worldwide every year and damage lives and property. Weather events like turbulence, strong wind over mountains, drainage winds, and Anabatic and Katabatic wind are also hazardous for aviation purposes. Many

researchers and scientists used various global to regional models for the better prediction of these events and to reduce damage related to such types of events. The global model has been used in many studies to find out the quantitative analysis of the extreme rainfall event as well as to understand the small and large-scale circulation patterns, but global models are not able to signify the meso to synoptic scale features of the heavy to extreme precipitation which is because of their coarse resolution. Therefore, regional models can simulate features of such types of extreme events as relations between topography and meso- synoptic-scale weather phenomena and give more reliable results (Chawla et al., 2018).

Among the many regional models, WRF is one of the numerical weather predictions (NWP) models and it has a wide range of applications from small scale to synoptic scale. To predict extreme events WRF is common because it has multiple physical options, users can adjust WRF for precise scales, topographical locations, and applications (Zeyaeyan et al., 2017). To predict extreme events weather the NWP was developed as a tool (Tanessong et al., 2017). The WRF is a regional popular community model widely used in both research and operational variety of meteorological purposes; to study the atmospheric dynamics such as thunderstorms, cyclones, extreme precipitation, hailstorm, etc. Globally, many studies have been done using the weather research and forecasting models some of them are; (Cardoso et al., 2013) used WRF to study simulation of mean and extreme precipitation climate over Iberian (Gelpi et al., 2016) used NWP parameterizations for the extreme precipitation events over Basque Country. Ntwali et al., 2016 apply WRF to study the topographical impact on spatial and temporal rainfall distribution over Rwanda. The study was done by (Avolio & Federico, 2018) using WRF for the simulations of heavy rainfall events in southern Italy. (Jee & Kim, 2017) studied the Sensitivity test of WRF for a Heavy Rainfall Event. Afandi et al., 2013 did a simulation over the Sinai Peninsula of heavy rainfall using the Weather Research and Forecasting model. Research by (Cassola et al., 2015) on numerical simulations of heavy precipitation events with the WRF model in the Mediterranean region. Moya-Álvarez et al., 2018 also studied the extreme rainfall in the Central Andes of Peru using the WRF-ARW Model. (Dasari & Salgado, 2015) studied the heavy rainfall simulation using WRF-ARW over the Red Sea region.

2.3 WRF in South Asia

Numerous studies have used the WRF model to simulate extreme events in their respected areas for accurate and timely prediction. Among the various extreme events here only focused on the extreme precipitation events because, in the recent decade, both frequencies of occurrence and intensity of heavy rainfall events over the Indian subcontinent are increasing (Singh et al., 2018). There are several studies done in the south Asian region using the numerical WRF model. Some studies with WRF are; (Kumar et al., 2012) used the WRF model for the simulation of the cloudburst event over the north-western Himalayan belt. Chevuturi et al., 2015 used the WRF model to simulate the heavy precipitation event in the central Himalayas. (Medina et al., 2010) applied the WRF model in the western and eastern Himalayas to find out the role of topography and land surface in the extreme convection. (Rajeevan et al., 2010) also used the WRF model for the simulations of a severe thunderstorm event over Southeast India and to examine the sensitivity microphysics scheme. The study by (Kar & Tiwari, 2016) used WRF to simulate the extreme rainfall events over Kashmir. To study the synoptic flow patterns and large-scale characteristics of rainstorms over northeast Bangladesh (Das et al., 2019) used the WRF model. similarly, the research was done by (ALAM, 2014) and also used the WRF for the simulation of heavy rainfall events in October 2007 over Bangladesh. In the past, many studies presented that for the simulation of devastating weather systems like extreme rainfall which leads to flood and landslide incidents over South Asia, (Das et al., 2019) said that the mesoscale models such as WRF are capable. Some of the study done by using the regional mesoscale model has revealed that the numerical model simulated the quantity of rainfall quite well with the observation. Many of the studies done in the Indian subcontinent region mentioned that the favorable synoptic situation related to heavy rainfall over north India and Nepal during the monsoon season, such as the moisture flux transport from the Bay of Bengal and the Arabian Sea by southeasterly and southwesterly flows, respectively, is necessary for the occurrence of thunderstorms and heavy precipitation To study small and large characteristics of intensely impacted extreme rainfall events, it is important to simulate such extreme events with the convective system using NWP model suitable for the region and to find out the better result.

2.4 WRF Aviation in Nepal

Spatiotemporal distribution of mesoscale phenomena arising in the Himalayans can simulate by the WRF-ARW model (Karki et al., 2018; Norris et al., 2015; Regmi & Maharjan, 2015; Shrestha et al., 2017). The complex land topography, lack of observational data, and remoteness in the Upper Himalayans are the main challenge for monitoring and forecasting extreme weather events. (Chawla et al., 2018). Flight-vulnerability assessment over a highly convoluted Himalayan Terrain using the WRF-ARW model can capture the formation of Cumulonimbus activity during the South-West Monsoon Season (Chandra et al., 2020). In the past, just a few experiments using the NWP model have been done for high-impact weather events over the different regions of Nepal. (Karki et al., 2018) studied the simulation of an extreme precipitation event over the Central Himalayas using the WRF model to find out the atmospheric mechanisms and their representation. Similarly, (Shrestha et al., 2017) did the sensitivity test of different WRF cloud microphysics of a Convective Storm over Nepal. (Orr et al., 2017) also studied the sensitivity of summer monsoonal precipitation in Langtang valley of the central Himalayas using the WRF model. One of the studies done by (Karki, et al., 2017) presented that the WRF simulated precipitation pattern at high resolution at 5km and 1 over the central Himalayas which visibly differentiates the mountain and valley precipitation. Hence, simulating precipitation patterns use of high resolution should be fruitful.

CHAPTER-III

MATERIALS AND METHODS

3.1 Study Area

Nepal is located in the transition between the Tibetian Plateau and the Indo-Gangetic plain along the southern slope of the Himalayas. It is bounded by the People's Republic of China in the North and India in the east, south, and west with the latitudinal and longitudinal bound of $26^0$22'N-$30^0$27'N, $80^0$40'E-$88^0$12'E respectively. With a total land area of 147,181 km², Nepal extends from east to west for about 885 km with a width of 145 to 245 km from north to south. Nepal is primarily a mountainous country characterized by diverse and extreme relief features and climate conditions. Traditionally, it is divided into three physiographic regions: terai, mid-hills, and high himalaya, each of which runs across the country from east to west. The altitudinal difference ranges from 59m to 8848.86m (Mt. Sagarmatha) above sea level. The study was considered as Taplejung district with an area of 3646 kilometers which is located in eastern Nepal in Province no 1. Geographically, Taplejung is a mountainous region with the highest peak Mount Kanchanjunga (8586m) which is located at a latitude of 27º 06' to 27º 55'N and a longitude of 87º57' to 87º40' E with an altitude range from 520m to 8586m above sea level. Within this elevation, there are five types of climate found from sub-tropical to polar climate. The event has happened in the Sisne Khola of the Pathivara Peak which is shown in Figure 4 indicated as a red dot. Pathivara is located at an altitude of 3794m from sea level. Figure 3 shows the selected study, domain for this study showing the accident site as black star dots.

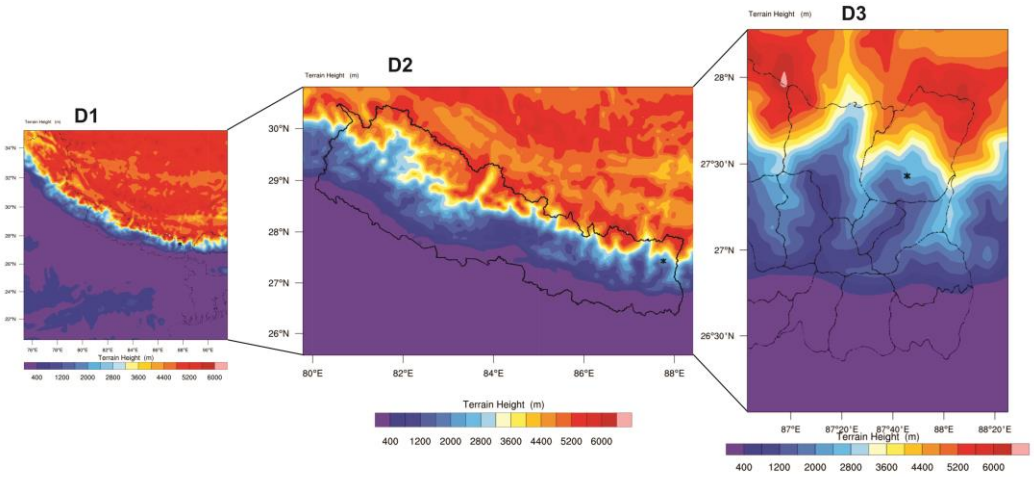

Figure 3: Selected Study domains D_1 (9 km), D_2 (3 km), and D_3 (1 km)

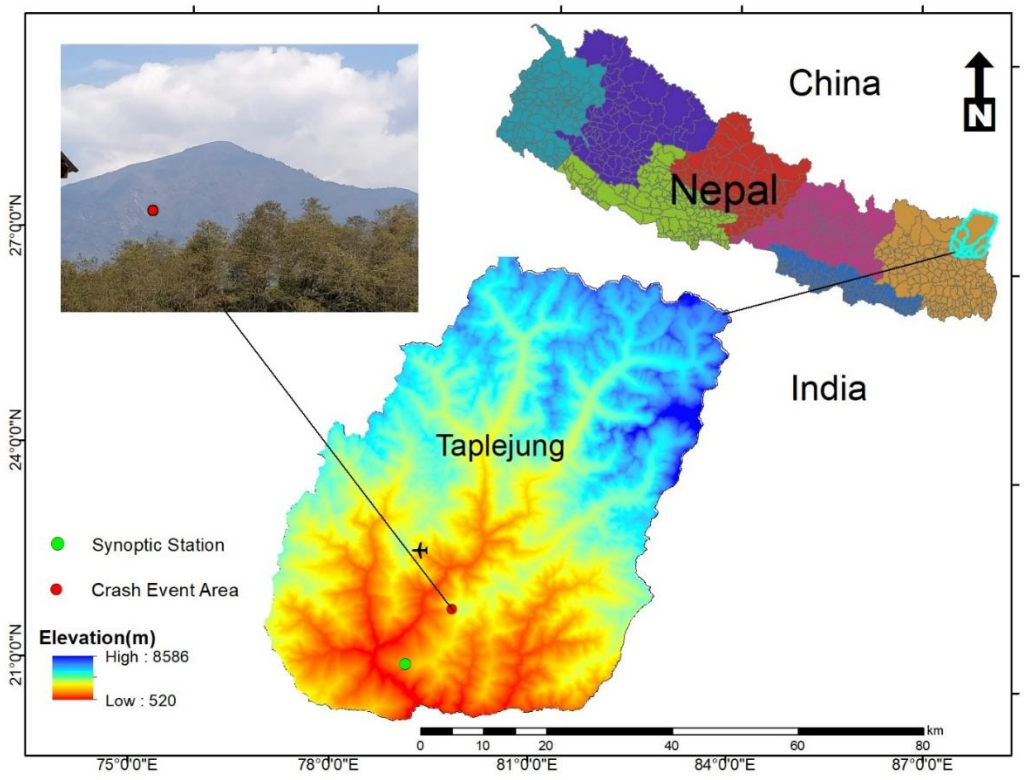

Figure 4: The study area is enclosed with the Taplejung district with the map of Nepal. The left-hand picture shows the Pathivara Peak with a red dot showing the accident site. (PC: Saroj Pudasainee)

3.2 Data

The research work is carried out using the data provided by meteorological stations (DHM), INSAT satellite imageries, and reanalysis datasets NCEP.

3.2.1 Initial and Boundary Conditions

The global six-hourly high resolutions (1° × 1°) National Centers for Environmental Prediction (NCEP FNL) datasets were obtained from the Research Data Archive of NCAR/UCAR (https://rda.ucar.edu/datasets/ds083.2/). That has been used as initial and boundary conditions of the WRF model. The lateral boundary conditions in the WRF model are updated at 6h intervals.The FNL data is the result of the same model which NCEP uses in the Global Forecast System (GFS), FNL is the final analysis, and delayed a bit from GFS is initialized so that they can include all of the available observational data. For time-dependent forecast needs, the GFS is run which uses FNL from the previous 6-hour cycle for initialization. The data is available from 1000 hPa to 10 hPa on the surface and 26 vertical levels. Parameters included are surface pressure, sea level pressure, geopotential height, temperature, relative humidity, u- and v- winds, vertical motion, sea surface temperature, soil values, ice cover, vorticity, and ozone. The archives are continuously updated to a near-current date if not maintained in real-time (*NCEP GDAS/FNL 0.25 Degree Global Tropospheric Analyses and Forecast Grids*, 2020)

3.2.2 In-situ observation

The Department of Hydrology and Meteorology is the official body of the Nepal Government that provides the hydro-meteorological data for the study. Rainfall data from the Taplejung (synoptic), Illam Tea Estate, Memeng Jagat, Lungtung station are used in the study. The available meteorological information provided by the Taplejung synoptic station is used for the comparison of model output. The AWS data was not available for the region. For comparison of vertical profile Gorakhpur Radiosonde station is used.

3.2.3 INSAT-3D

The INSAT-3D Daily infrared images available are used to know the atmospheric condition at the time of the event. INSAT-3D is an exclusive mission designed for enhanced meteorological observations and monitoring of land and ocean surfaces for

weather forecasting and disaster warning. INSAT-3D is the first Indian geostationary satellite, equipped with a sounder instrument. INSAT-3D satellite provides a wide range of atmospheric products such as cloud coverage images, atmospheric winds, sea, and land surface temperatures, humidity, quantitative rainfall, earth's radiation, atmospheric profiles, ozone, atmospheric stability parameters, fog, and snow, aerosols over Indian landmass and adjoining areas. These products are immensely helpful in monitoring day-to-day weather and predicting extreme events like tropical cyclones, thunderstorms, cloud bursts, and heatwaves. The INSAT-3D Imager is an upgraded version of the Very High-Resolution Radiometer instrument of the Kalpana-1 and INSAT-3A missions (Navale et al., 2020). These satellites have an imaging system that provides images in Visible, Near Infrared, Shortwave Infrared, Water Vapor, and Thermal infrared band. (*Insat-3d-Brochure.Pdf*, n d.)
https://www.isro.gov.in/sites/default/files/article-files/node/7954/insat-3d-brochure.pdf

3.3 Model description and Experiment design

3.3.1 Weather Research and Forecasting model

The Advanced Research Weather Research and Forecasting (ARW-WRF) model, version 4.0.3 is used for the event. The Weather Research and Forecasting (WRF) is a fully compressible, three-dimensional, eulerian, non-hydrostatic model with multiple nesting options (Skamarock et al., 2019).

- The WRF Preprocessing System (WPS)
- Dynamic solver
- Post-processing and visualization

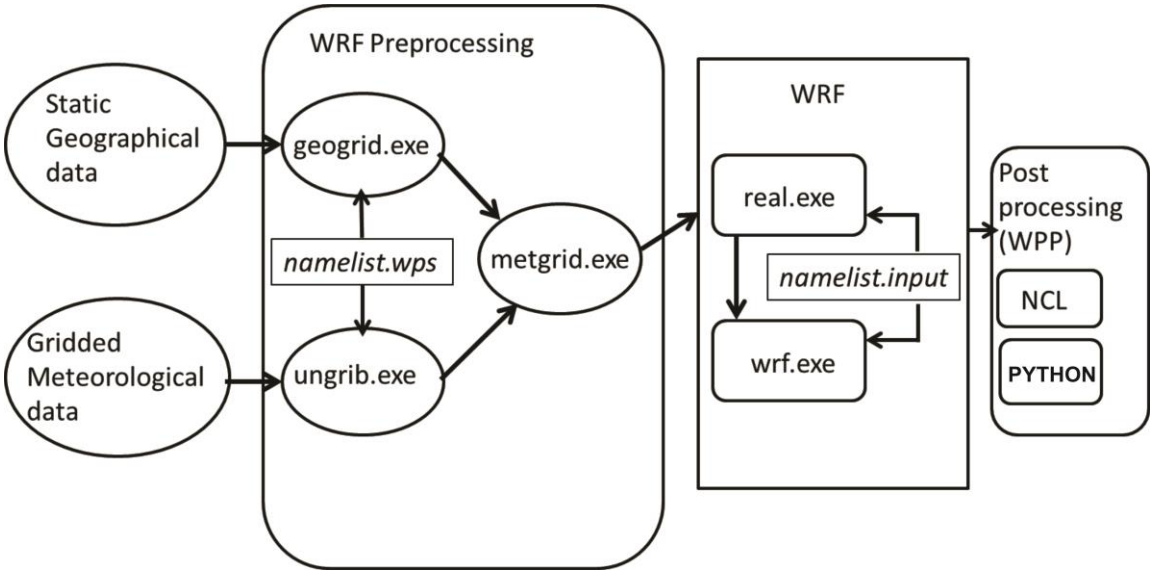

Figure 5: WRF-ARW workflow

3.3.2 WRF Preprocessing System

WPS is a program used for real data simulation. Its function is to prepare input for a real program. It has three sets of the program (geogrid.exe, ungrib.exe, and metgrid.exe) which are briefly described below: (Figure 5)

Geogrid .exe: The main drive of this program is to define the simulation domain and interpolate the various static terrestrial datasets to the model grid. The several terrestrial datasets include soil categories, land use category, terrain height, vegetation cover, albedo, etc. These datasets are interpolated to the model grids. Besides interpolating the default terrestrial fields, it can also be able to interpolate various continuous and categorical fields to the simulation domains.

Ungrib.exe: The GRIB files are used in the ungrib program which describes the data and saves these data in the intermediate format, which can then use in the met grid program. It includes numerous meteorological fields such as temperature, precipitation u-, v-, w winds, sea level pressure, surface pressure, etc. which are from different global to regional models like NCEP GFS. The ungrib program can read GRIB1 and GRIB2 files. Here, in this study, we used GRIB2 files which use various codes to identify the variables and levels.

Metgrid.exe: The met grid program horizontally interpolates fields that are obtained from geogrid and ungrib programs to the selected simulation domains. This interpolated

met grid output can then be taken by the real.exe program of WRF. The work of the met grid program is time-dependent and runs every time a new simulation is initialized like ungrib program. (*ARWUsersGuide.Pdf*,n.d.)
http://homepages.see.leeds.ac.uk/~lecrrb/wrf/aRWUsersGuide.pdf

3.3.3 WRF

After WPS ran successfully, the WRF model is ready to run and the model contains a different initialization program (real.exe) and a numerical integration program (wrf.exe). The initial and boundary condition for the wrf.exe portion is generated by the real.exe portion of the program that is derived from the output files provided by the WRF Preprocessing System (WPS). The real.exe program completes the following work:

- Read data from the name list of WPS and allocate space
- Initialize the rest of the variables
- Read input data from the WRF Preprocessing System (WPS)
- Prepare soil fields for use in the model (usually, vertical interpolation to the requested levels)
- Checks to verify soil categories, land use, land mask, soil temperature, and sea surface temperature are all consistent with each other
- Generate the initial and lateral boundary conditions files

After running the real.exe program, the numerical integration program i.e., wrf.exe can be able to run which is used to provide prediction/forecast over a specific duration. For this it takes the initial and boundary condition provided by the WPS, these will be directly used by the WRF model. The setting in the name list. The input file should be the same as the namelist.wps file for the configuration of the WRF model. (*ARWUsersGuide.Pdf*, n.d.)

3.3.4 Experimental design

The model was initialized with meteorological data from the operational analysis performed every 6 hour at the National Centers for Environmental Prediction (NCEP Final Analysis) and the 24-category land-use and default terrain elevation data of the U.S. Geological Survey (USGS). The simulation was carried out for the period of 0600 UTC (11:45 LST) from 26 February to 0600 UTC (11:45 LST) on 28 February 2019

with WRF, version 4.0.3. The Thompson graupel scheme (Thompson et al., 2004) for microphysics, RRTM scheme (Mlawer et al., 1997) for longwave radiation, Dudhia scheme (Dudhia, 1989) for shortwave radiation, Mellor Yamada Janjic (MYJ) scheme (Janić, Z. I., 2001)for the planetary boundary layer, and the Noah land surface model (F. Chen & Dudhia, 2001) have been used for the calculation. The WRF output history interval was set at 15min. A brief description of the model configuration is given in Table 2.

Table 2: Model setup and configuration

Physics/domain design	Parameterizations used
WRF Model version	4.0.3
Domain System	Triply nested two-way interaction
Domain Center	27.5^0 N, 87.7^0 E
Horizontal resolution	9km × 3km × 1km
Horizontal grid points	91 × 91
Vertical grid points	40
Model top	50 hPa
Microphysics	Thompson graupel scheme
Longwave radiation	RRTM
Shortwave radiation	Dudhia scheme
Land surface model	Noah
Planetary boundary layer	MYJ
Boundary data	NCEP FNL
Land use	24-category USGS
Start date	06 00 UTC 26 Feb 2019
End date	06 00 UTC 28 Feb 2019
Output history interval	15 min

Moreover, several test simulations were carried out for three different days with 15-min output history intervals with different physics options as well as vertical grid points and 40 vertical levels. The whole work is carried out in the climate and atmospheric modeling lab of the Central Department of Hydrology and Meteorology. (CDHM)

Figure 6 shows the Domain confurigation for this study. D_1 (9km) is the coarse domain, D_2 (3km) is the fine domain, and D_3 (1km) is the finest domain. The finest domain is used for the meteorological analysis located in Eastern Nepal whereas the coarse domain is used for a synoptic condition over Nepal during the time of the accident.

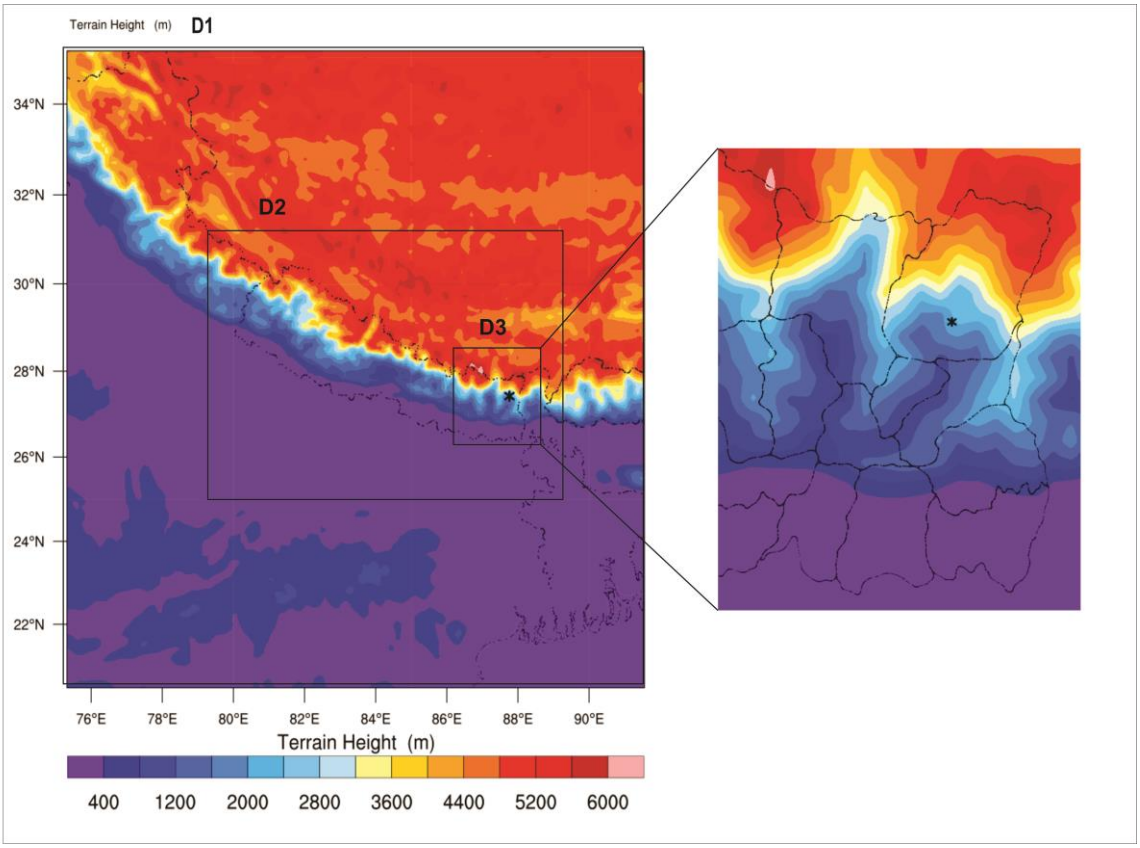

Figure 6: Illustration for the 3 nested domains D_1 (9 km), D_2 (3 km), and D_3 (1 km) with D_3 over Eastern Nepal, Taplejung used for model simulations

CHAPTER-IV

RESULTS AND DISCUSSION

4.1 Results

In the following subsections, we describe the model validation and variation of several meteorological fields, particularly close to the time of the accident when the helicopter (aircraft) went missing, and examine if they played any deterministic role in the fatal accident.

4.1.1 Model validation and overview of local weather

We are not able to give the desired quantitative validation of model prediction because the aircraft accident site lacks Automatic Weather Station (AWS) data. There are a few manually collected meteorological surface observations (such as maximum and minimum temperatures, relative humidity, and rainfall) that we can use to assess the reliability of model predictions. Although the model predictions for certain meteorological variables closely matched the observed patterns. (Figure 7a–d)

For maximum and minimum temperatures, the model slightly overestimates the observed value in both the Taplejung and Illam Tea Estate stations. In the case of relative humidity at 3 UTC over Taplejung station, both observed and model calculated were given accurate readings, while at 12 UTC, the results were underestimated. The observed and calculated relative humidity were overestimated at the Illam Tea Estate station. D_1 contains four precipitation stations, including one synoptic station (Figure 7d). All stations recorded moderate rainfall in the 24 hour accumulated period on February 27, 2019. Taplejung and Illam Tea Estate stations overestimate, while Lungtung and Memeng Jagat stations underestimate rainfall.

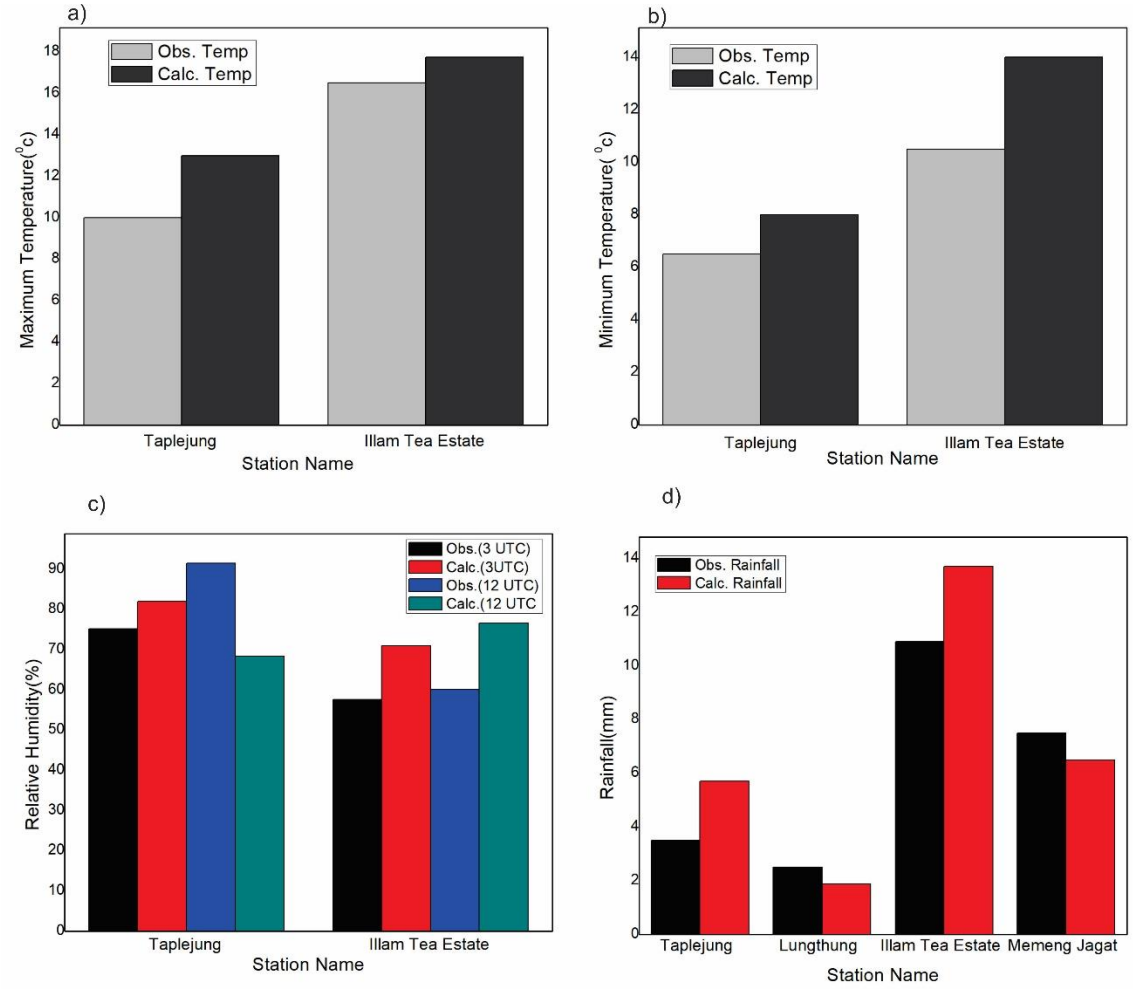

Figure 7: Comparison of observed and calculated (a) daily maximum temperature (b) daily minimum temperature (c) relative humidity and (d) rainfall at a different station

4.1.2 Precipitiable Water

The depth of water in the atmosphere is measured in its column. Its value has great importance in the behavior of the atmosphere. The amount of precipitable water in the atmosphere is linked with the rain. Figure 8 shows the spatial and temporal distribution of precipitable water over Nepal. At 5:45 LST, the water vapour level at the accident site was around 8 kg/m2, but by 12:30 LST, it had risen to around 20 kg/m2. The precipitable water also indicates that the weather over Eastern Nepal was unfavorable during the time of the helicopter crash.

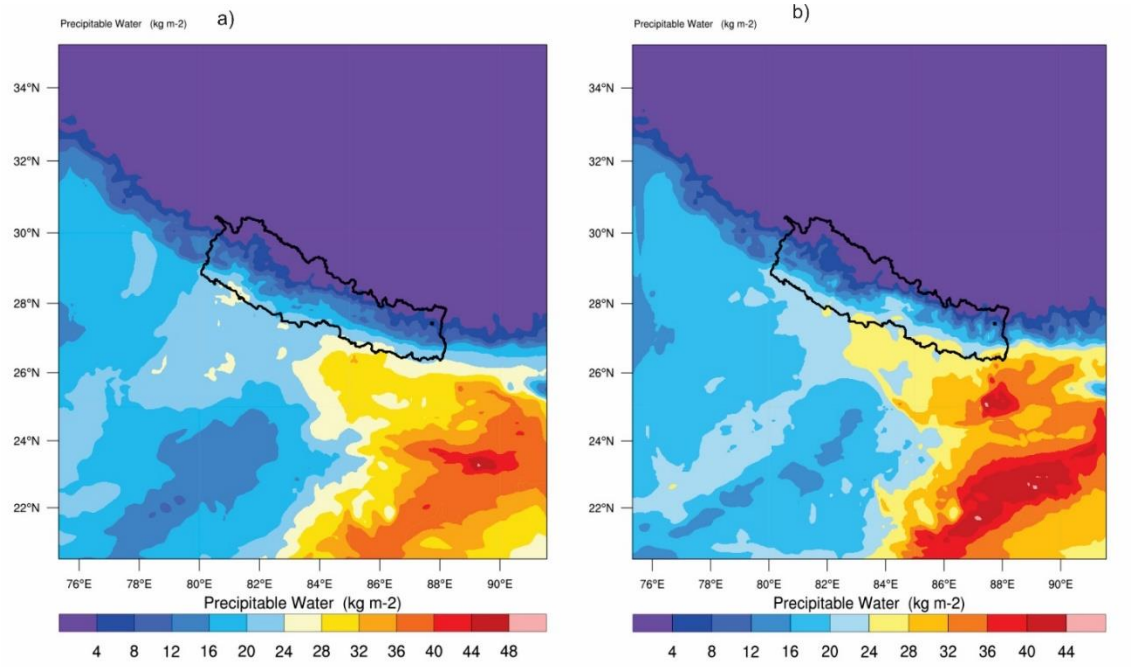

Figure 8: Spatial and temporal distribution of Precipitable water over Nepal .a) 5:45 LST b) 12:30 LST

4.1.3 Accumulated Precipitation

Precipitation is the deposition of atmospheric moisture on the Earth's surface. Atmospheric moisture may be precipitated either in solid or liquid forms, for example, rain, snow, drizzling, glazing, hail, sleet, and dew.

During winter, Nepalese weather is influenced by western disturbances. Figure 9 (a-b) shows the accumulated rainfall and snowfall over 24 hours by WRF simulations. The model captures the events that occurred in most of the central region and some parts of the eastern region. From this plot on the accident date, the eastern mountainous region has moderate snowfall. The real-time picture (Figure 13) also illustrates this snowfall event.

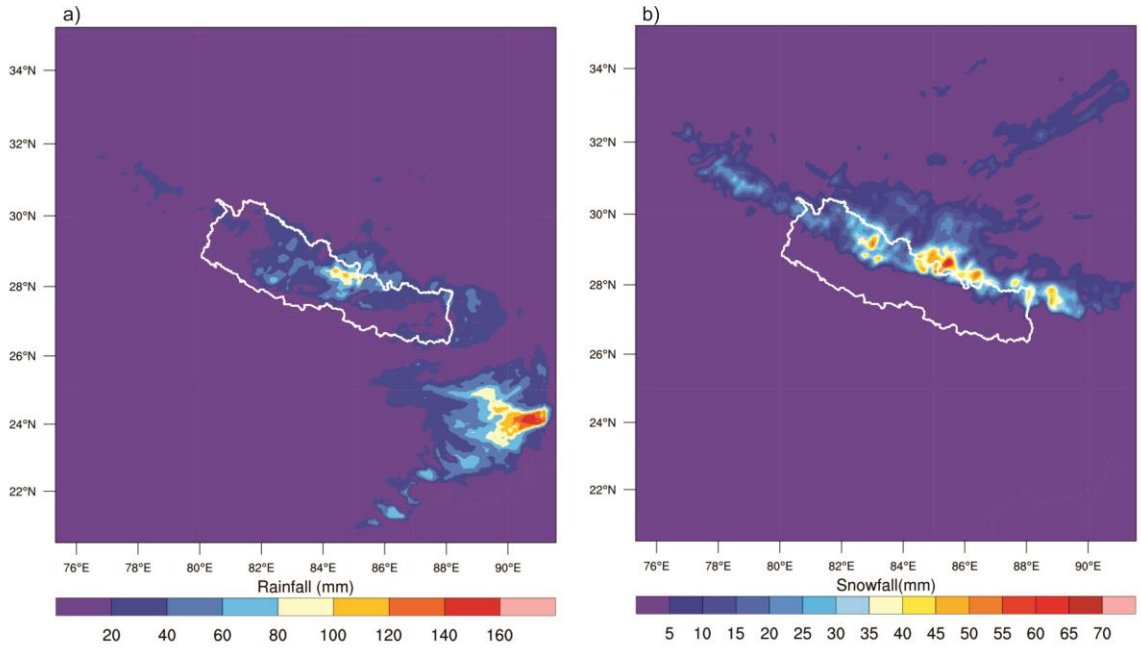

Figure 9: 24-hour accumulated precipitation from WRF simulation (a) Accumulated Rainfall (B) Accumulated Snowfall over Nepal

4.1.4 Synoptic Analysis

The absence of meteorological observations in and around the aircraft accident site prevents us from presenting the desired quantitative validation of model predictions of surface winds with sea level pressure over Nepal shown in Figure (10 a - d). The spatial and temporal distribution of surface wind over D_1 shows that there is convergence over North India along with low pressure.

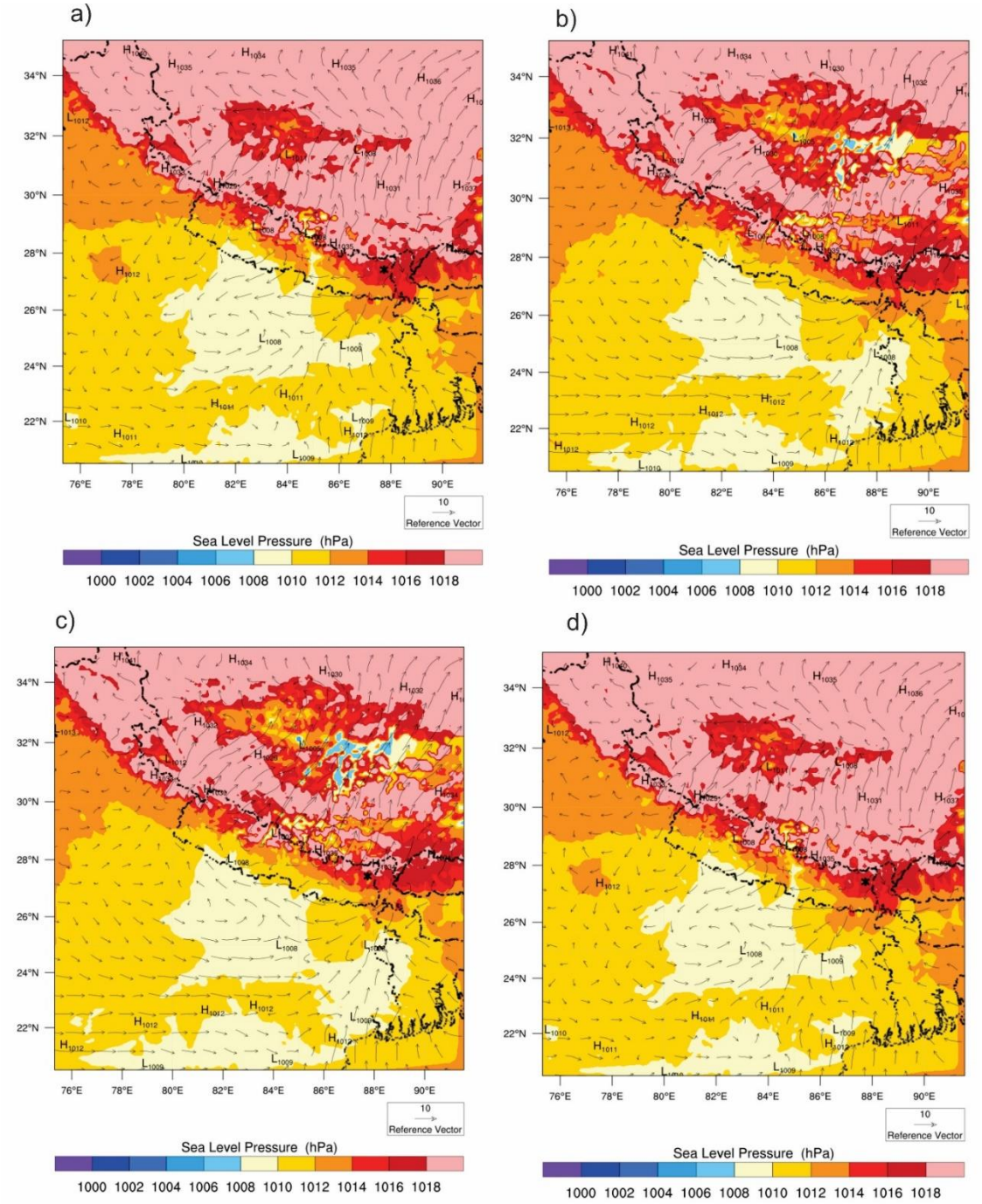

Figure 10: Sea level pressure and surface winds over D_2 (a) 5:45 LST (b) 12:30 LST (c) 12:45 LST and (d) 17:45 LST

The surface map analysis at 12:45 LST shows a low-pressure area over North Central India and the south of Eastern Nepal and Western Nepal. The low-pressure system supported the flow of warm and moist air from the Mediterranean Sea and westerly flow over Nepal. The weather over Nepal from the western part was disturbed by the impact of the western disturbance. The winds flowing over the mountainous region of Nepal create turbulence over the accident site.

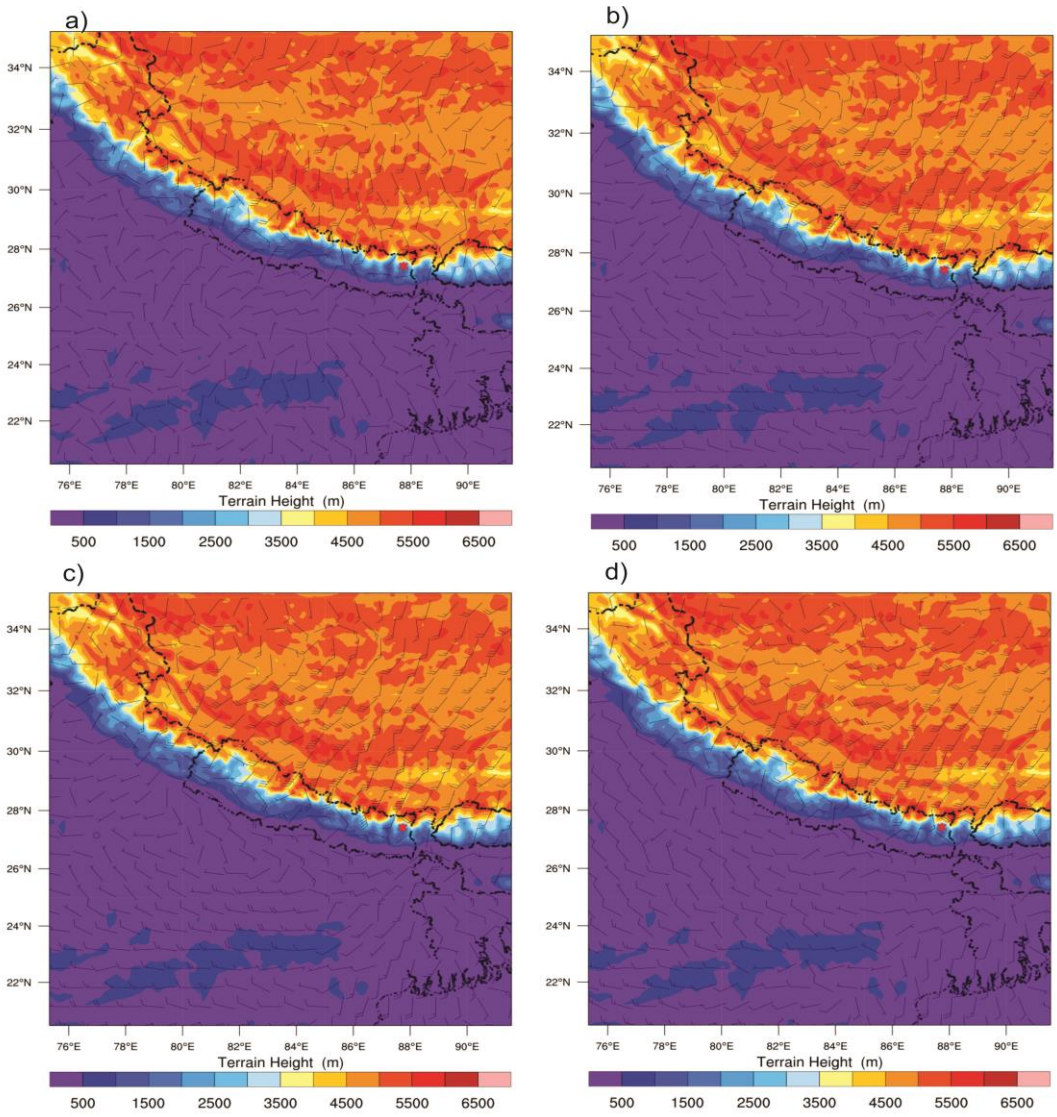

Figure 11: Near-surface flows in Coarse Domain (D_1) (a) 5:45 LST (b) 12:30 LST (c) 12:45 LST and (d) 17:45 LST, red dots show the accident sites

4.1.5 Geopotential Height

Geopotential height approximates the actual height of the pressure surface above mean level. It is also the amount of work that would have to be done, against the force of gravity, to lift a unit mass to that location from mean sea level. Troughs and ridges become distinctive with a geopotential height plot of constant pressure level. The large scale forcing (synoptic flow pattern) along with the geopotential height of domain D_1 grid spacing at 500 hPa and 300 hPa are presented in Figure 12. On average, the 500 hPa level is around 5.5 km amsl. Figure 12a shows the southern slope has a high geopotential height, whereas the northern side has a low geopotential. The 500 hPa level is often referred to as a steering level because the underlying weather systems roughly move in the same direction as the winds at that level. At the time of the accident, at 500 hPa, about 40 knots of westerly wind were blowing along with the movement of underlying weather. The low geopotential indicates the low pressure where the high geopotential indicates the high pressure. This also indicates the middle tropospheric weather over our regions. The red dots show the exact location of the crash site. At 300 hPa, about 60 knots of westerly wind is blowing.

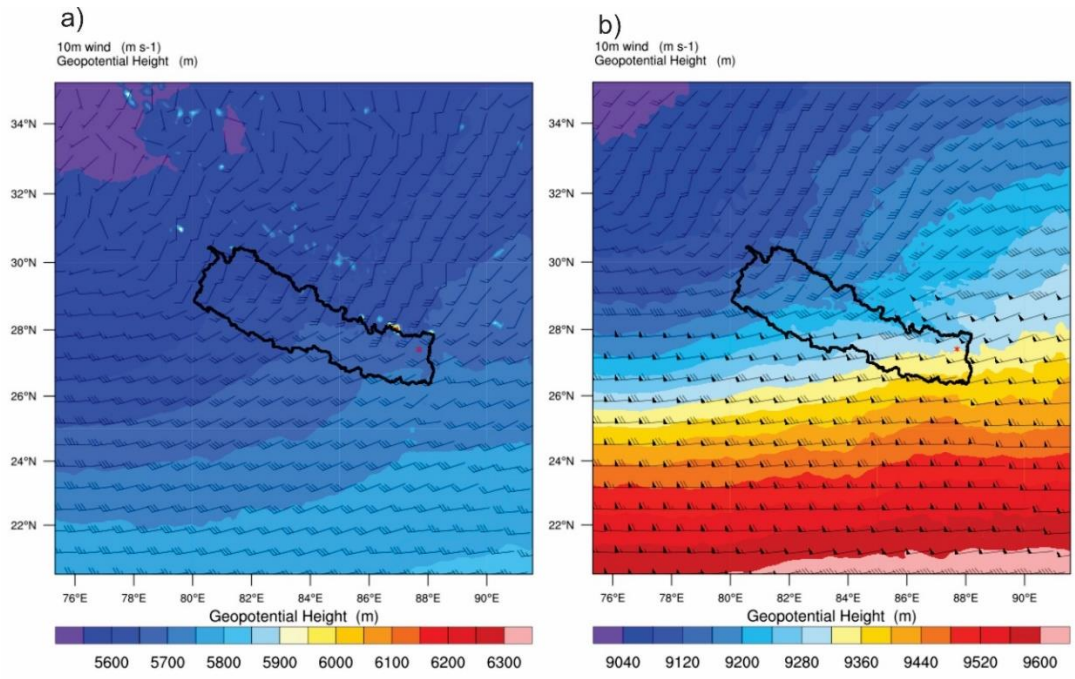

Figure 12: Geopotential height along with wind bar a) 500 hPa b) 300 hPa at accident time

4.1.6 Meteorological Information

The Department of Hydrology and Meteorology (DHM) is the official body to provide meteorological information. The weather at Kathmandu, en-route, and the accident site were provided by DHM. The real-time weather at Pathibhara Peak was received by interviewing the local people there and analyzing real-time photographs collected. (Helicopter accident investigation commission, 2020)

4.1.7 Weather Condition over Eastern Nepal

Forecast issued by Meteorological Forecasting Division, DHM, based on weather observations, weather charts, and satellite images. The weather condition over Eastern Nepal was as follows

Wind: At 6: 00 UTC (11:45 LST), the wind flow pattern at surface wind depicted easterly to southerly- easterly wind over Nepal. The high-altitude wind at 700 and 500 hPa showed south-westerly to southerly wind over the eastern side of Nepal at 6:00 UTC.

Figure 13: Air Dynasty Helicopter at Pathivara Helipad with Tourism Minister showing snow and low visibility (Source: Helicopter accident investigation commission, 2020)

4.1.8 INSAT-3D and Relative Humidity

INSAT-3D Infrared imageries of February 27 2019 at 12: 45 LST is shown in Figure 14a. The satellite images are taken from ((https://mosdac.gov.in/gallery/index.html?&prod=3DIMG_*_L1C_ASIA_MER_BIMG_NEPAL.jpg&date=2019-02-26&count=32#)

Satellite images show the development of thick clouds over Nepal and the adjoining area. The dense cloud covers over western and eastern regions during the accident of the Air Dynasty Helicopter. The 12:45 LST just a few min after the accident time the Eastern part of Nepal has dense clouds which are the driving factors supporting this accident. Rainfall is higher in the region with dense cloud mass and low in the region with few clouds mass shows that the observed rainfall is usually in good accord with satellite images

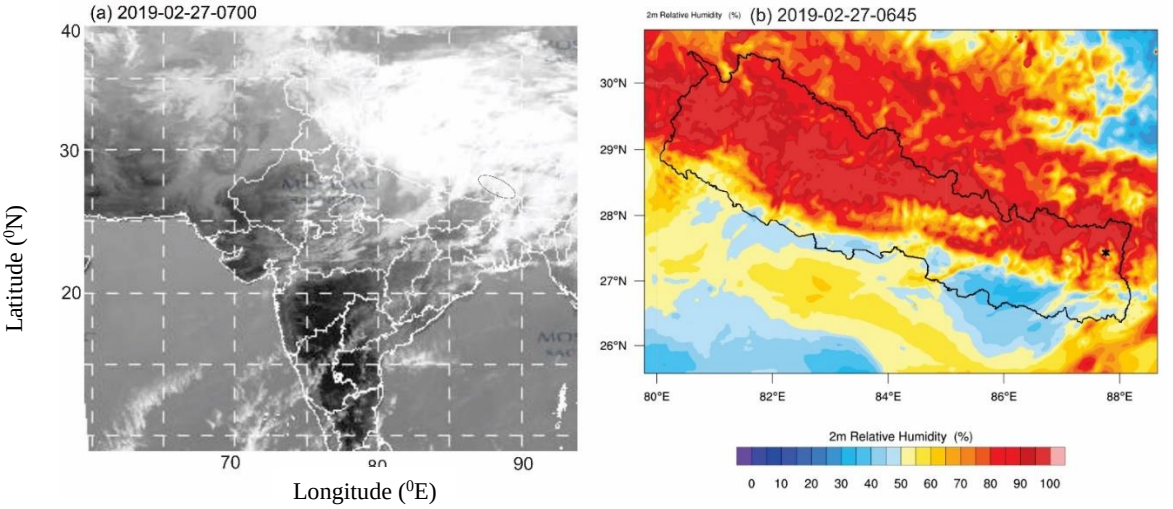

Figure 14 : (a) INSAT-3D Visible imageries of southern and (b) Relative Humidity during the time of accident 27 February 2019, black oval shows the crash site

On 2019-02-27 12:30 LST on the entire mountainous region has maximum relative humidity as per model simulations (Figure 14b). There is more than 90% relative humidity in eastern Nepal while low in comparatively low relative humidity over the lower altitude region. This implies during the time of the accident the air was humid which directly helps for the unstable atmosphere over the accident site.

4.1.9 Local Flow Characteristics

The characteristics of local flows show the meteorological condition of the region. Thus, understanding the spatial and temporal distribution of local flows over the area of interest is important to assess prevailing weather features and their impact. Figure 15 (a-d) shows the surface wind over terrain height in different time intervals. It seems more than 45knots south wisterly wind flowing at a high altitude and about 10 knots of winds flowing NE in the accident site and it was hazardous for helicopter at complex terrian. The red dot shows the exact accident site. The strong wind helps to blow snow in the upper regions that might be a region of snowfall in Pathivara Peak.

The horizontal distribution of surface wind over D_1 was nicely captured by the WRF model. This type of surface flow helps to identify the wind speed and direction over any local place. This surface wind information was very useful for aviation purposes and route forecasts. (Figure 11)

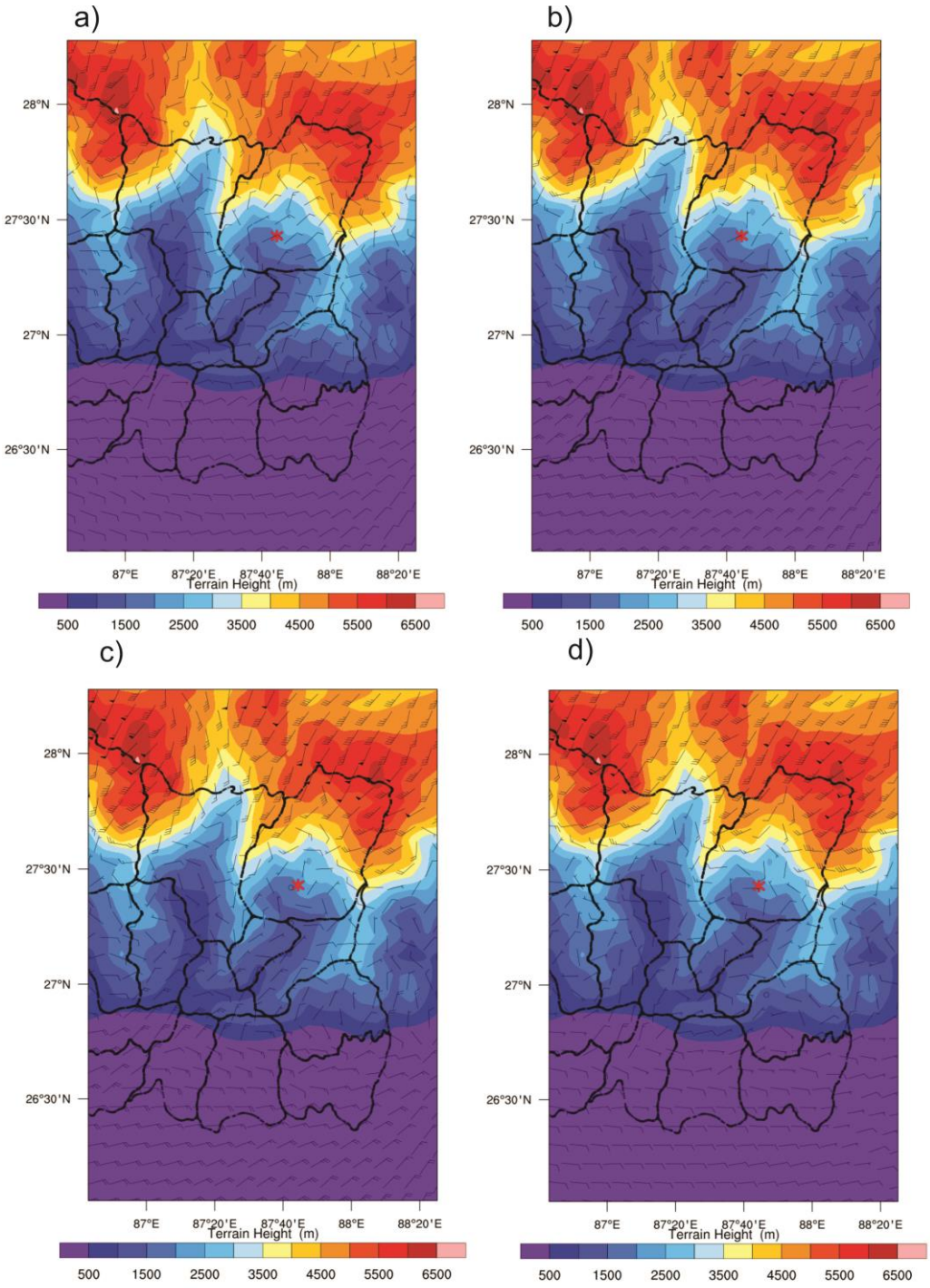

Figure 15 : Horizontal distribution of surface winds (a) 5:45 LST (b) 12:30 LST (c) 12:45 LST and (d) 17:45 LST in D_3

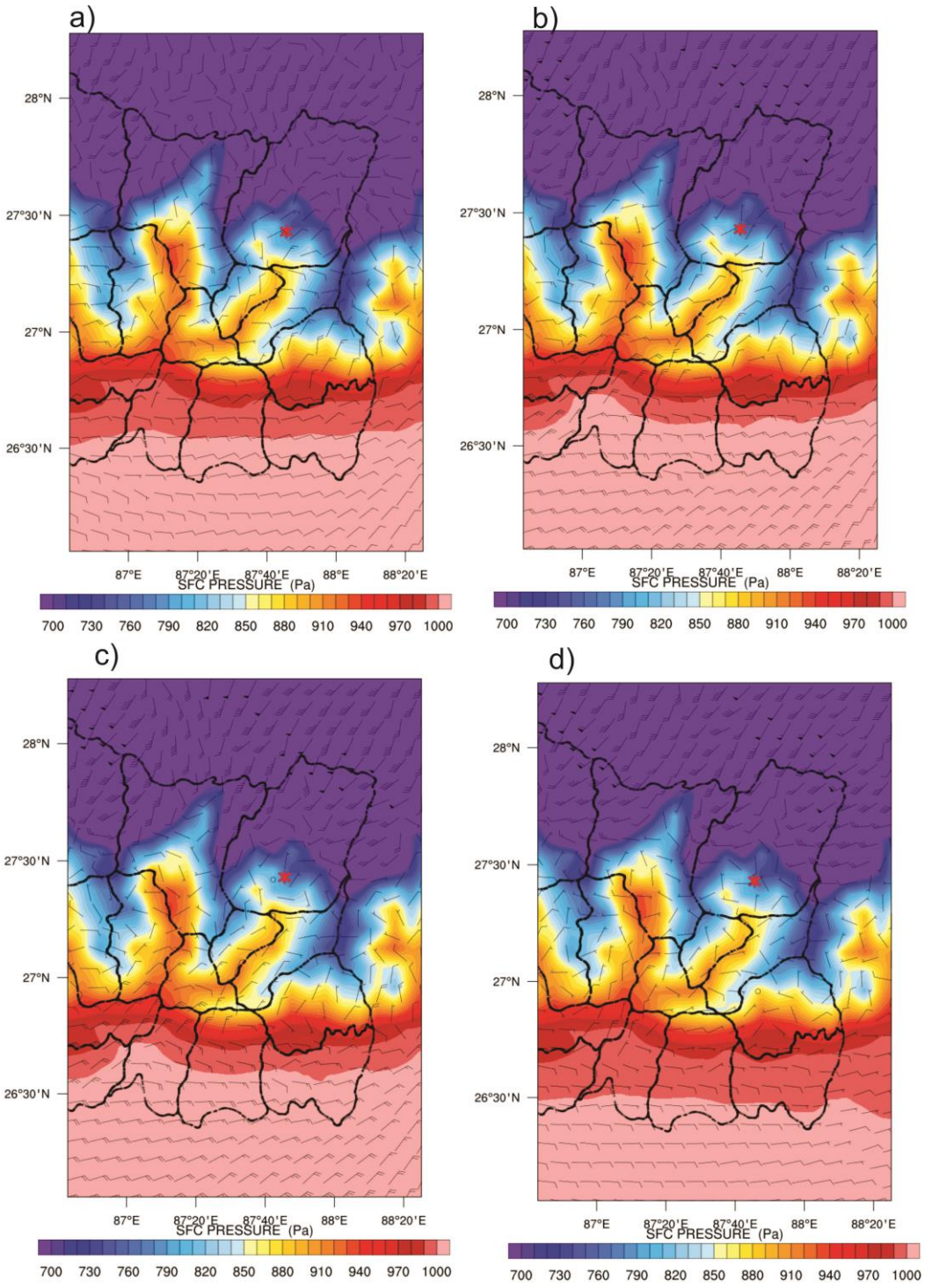

Figure 16: Horizontal distribution of Surface pressure (a) 5:45 LST (b) 12:30 LST (c) 12:45 LST and (d) 17:45 LST in D_3

Figure 16(a-d) shows that there is lower pressure compared with lower altitudes in the region but strong winds were flowing. The pressure ranges from 700 to 1000 Pascal. As strong winds around the complex terrain were hazardous for mountain flight. The

plots also determine surface pressure decreases with increasing altitude. The high-altitude region over the D_3 implies lower pressure. The lower atmospheric pressure is the key indicator of the unstable atmosphere over any region. The pressure chart, as well as such plots, helps to identify the surface pressure and the WRF model can capture the pressure over the flight route.

4.1.10 Vertical Cross Section of Reflectivity

The most obvious parameter that pilots look for is the RADAR reflectivity (V. V. Kumar et al., 2013; LeMone & Zipser, 1980; Sauvageot & Omar, 1987). Radar reflectivity contours provide valuable information on the microphysical properties of clouds, for instance, a radar eco (measured in dBZ) whose strength is directly proportional to the concentration and the radii of droplets, correlates directly with the intensity of the precipitation. (Matsuda & Onishi, 2019) show an increase in radar reflectivity factor over regions of high liquid water content (LWC), particularly over regions where a non-uniform distribution of droplets is observed. A large value of radar reflectivity is attributed to scattering by the higher concentration of droplets.

Figure 17 shows the vertical crosssection of reflectivity (dBZ) over the terrain. For this analysis, the weather research and forecasting model is used. A value more than 30 dBZ indicates heavy rainfall (H. Chen et al., 2021). During the time of the accident at 12:30 LST, the value of dBZ over the terrian was found as 25-35 dBZ which denotes there is an unfavorable atmospheric condition. These results identified and capture atmospheric condition over the complex terrain. The panel plot from Figure17 (a-d) also clearly shows that dBZ values range from between 20- 45 dBZ over the finest domain.

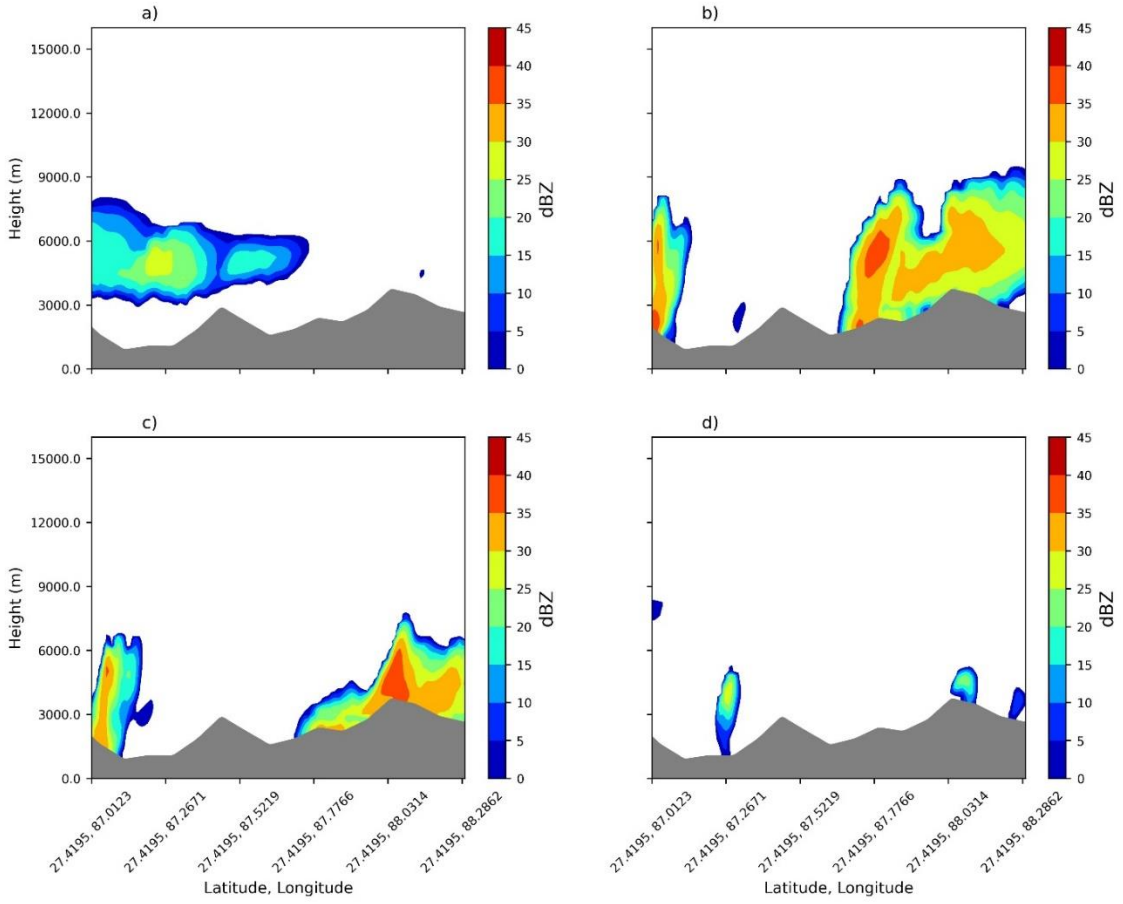

Figure 17: Vertical cross-sections of simulated reflectivity (dBZ) along the accident area obtained from the WRF model for the following times (a) 5:45 LST (b) 12:30 LST (c) 12:45 LST and (d) 17:45 LST in D_3

4.2 Hydrometeor Distributions Along with Accident Site

Hydrometeor characteristics along the flight path help to understand the risk of inflight icing. (Jarvis & Stuart, 2001). Inflight icing is determined to be a cause or factor for poor efficiency as well as for numerous fatal aircraft accidents(Ashenden & Marwitz, 1997; Marwitz, 2013). The hydrometeor condition along the flight path of 9N-AMI Air Dynasty Helicopter, we examine the vertical distribution of temperature, humidity, and cloud water and graupel mixing ratio in the cross-section along east-west direction keeping latitude constant at accident crash latitude (27.43N). (Figure 18)

4.2.1 Model Generated Isotherms

The vertical temperature profile drives cloud microphysics within moist air in the atmosphere. It is crucial also to look at isotherms along the accident area for analysis of the model hydrometeor profile. Figure 18 shows the temperature contours on the 19th of February 2019, spanning four-time intervals. Figure 18 (c), shows that at the accident site (27.43N, 87.74N), the temperature varies from (10 to -20) ^{o}C, a temperature band where warm rain microphysics dominated. At an altitude of 3000 m MSL, the vertical temperature was noted to be (0 to -10) ^{o}C, which is sufficient enough to form snow and cold ice-driven microphysics. The cross-section of temperature shows that the altitude of the accident site (3154 m MSL), which just lies below the Pathivara Peak (3794 m MSL), persistently has the temperature at or below the freezing point. This shows that during the times of the accident, the entire area was cold and the above model performance also illustrates that moderate snowfall occurred in the surrounding area, which may have caused the inflight icing for the helicopter accident

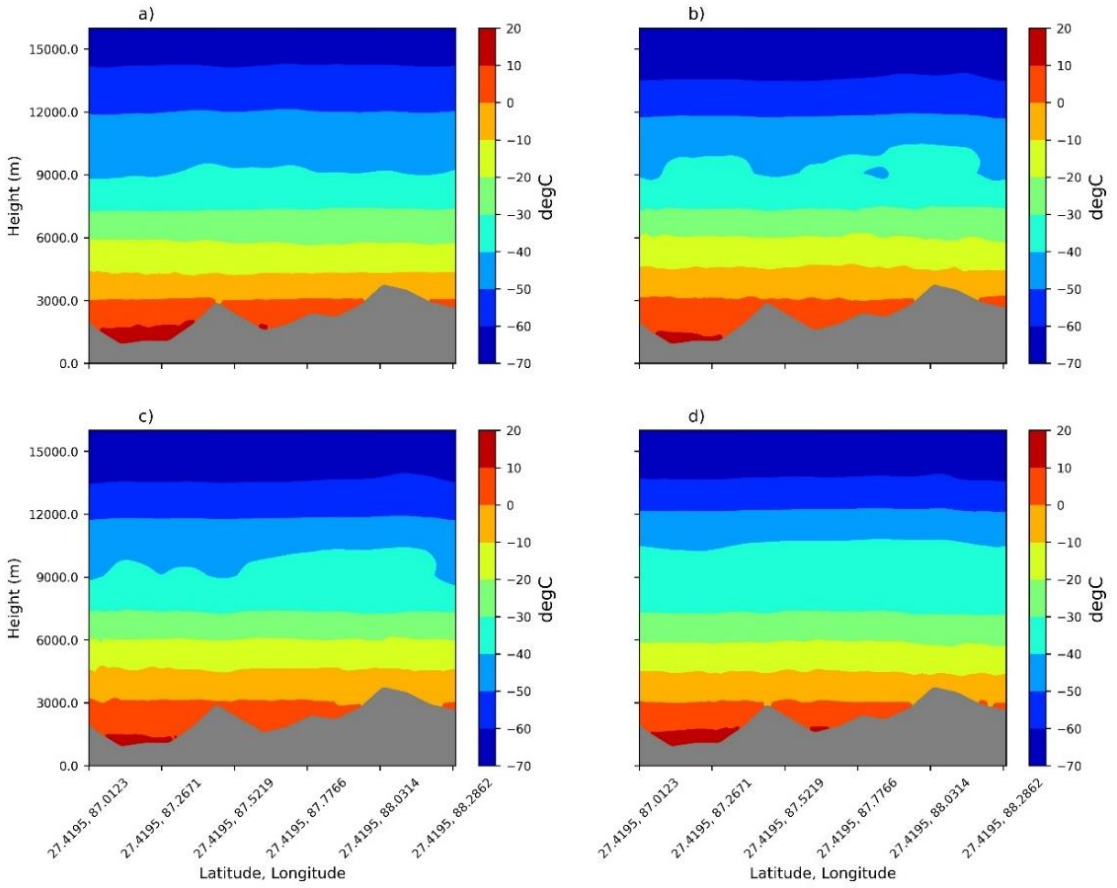

Figure 18: Model-generated Isotherms on the 27 Feb 2019 for the following times (a) 5:45 LST (b) 12:30 LST (c) 12:45 LST and (d) 17:45 LST in D_3

4.2.2 Diurnal Variation of Temperature

Figure 19 shows the diurnal temperature variation at different pressure levels based on the reference point of the accident site. At 12:30 LST, the temperature is below freezing over the Pathivara Peak and the temperature is decreasing up to -19 ^{o}C at 500 hPa , -9 ^{o}C at 600 hPa and 0 ^{o}C at 700 hPa.

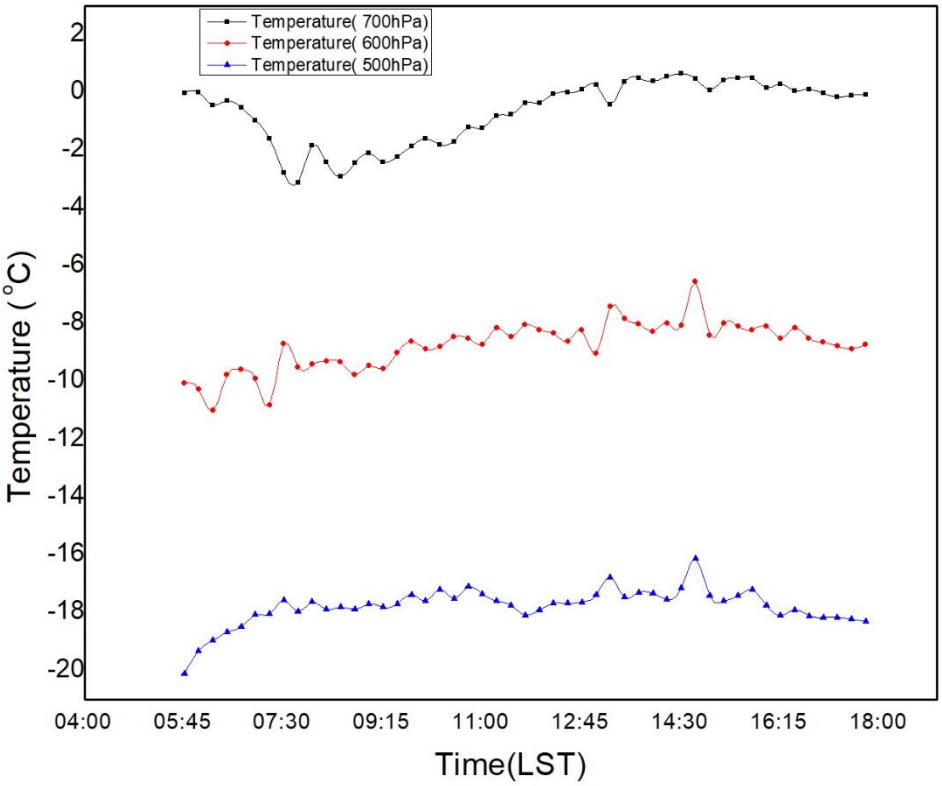

Figure 19: Diurnal variation of temperature at 700 hPa, 600 hPa and 500 hPa focusing the accident point

4.2.3 Vertical Cross Section of Cloud, Graupel, and Snow Mixing Ratio

Figure 20 shows the vertical cross-section of hydrometeor distributions along a west to east over the D_3 in two different time shots. Panel a and b shows the snow mixing ratio where the model captures a maximum of 2.0 g/kg snow, a very low amount of graupel, and a middle-level cloud mixing ratio during the time of the accident. These plots illustrate that a moderate amount of snowfall occurred during accident time over Eastern Nepal. When Super-cooled Liquid Droplets (SLD) in low-lying clouds make contact with aircraft parts exposed to oncoming air currents then a portion freezes immediately. It is quite likely that any non-frozen amounts trickled across the wings

causing a water film that eventually froze at the subzero temperatures of the underlying structure (Sand et al., 1984)

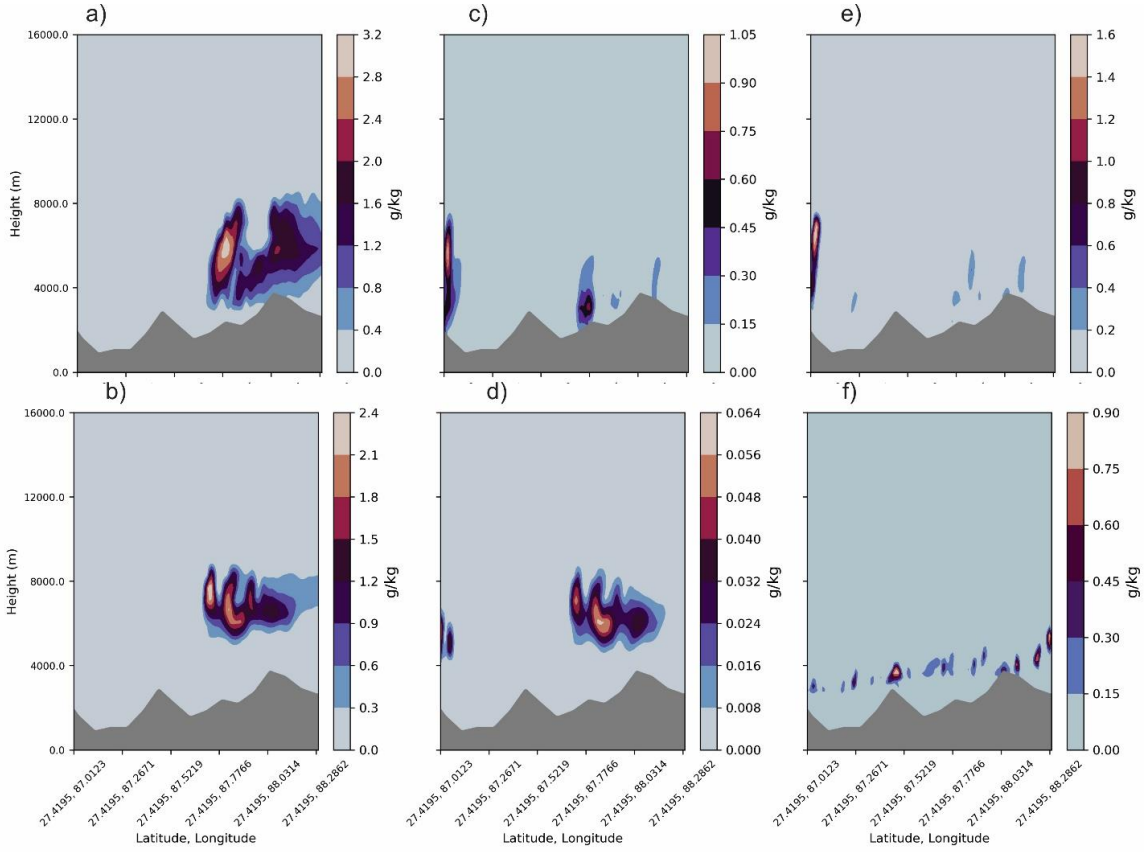

Figure 20: Vertical cross-section of (a-b) Snow mixing ratio (c-d) Graupel mixing ratio (e-f) Cloud mixing ratio at 12:30 and 12:45 LST

4.2.4 Vertical Cross Section of Relative Humidity

The vertical cross-sections of relative humidity are also provided below in Figure 21 (a-d) for 27 February at different time intervals. The relative humidity profile shows that a considerable level of humidity was present at 3000m MSL level in the range from 90% and above being advected by the westerlies (Figure 11). This (90-100) % relative humidity was present over accident areas. A high percentage of relative humidity infers that the air was nearly saturated and sufficient enough for the hydrometeor's formation. The WRF model simulation for the snow, graupel, and cloud mixing also illustrate that during the time of the accident sufficient moisture over the entire region. (Figure 20 e-f)

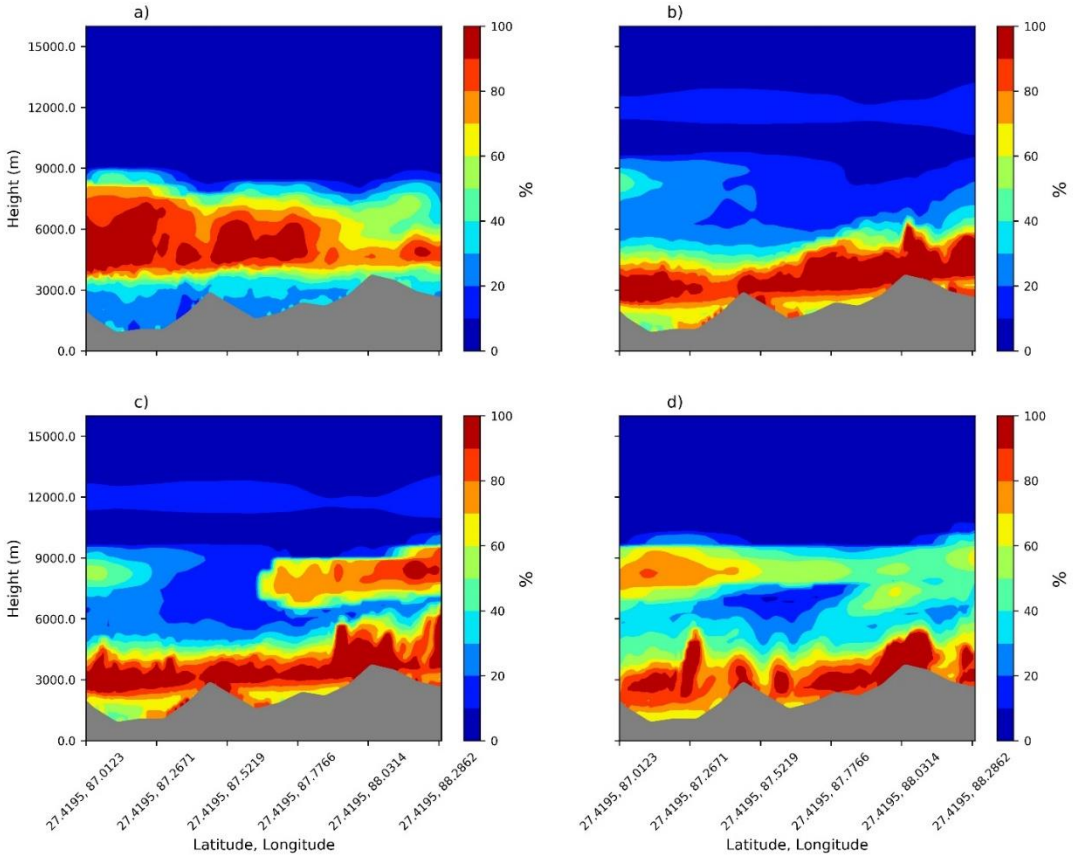

Figure 21: Vertical cross section of simulated relative humidity (a) 5:45 LST (b) 12:30 LST (c) 12:45 LST and (d) 17:45 LST in D_3

4.3 Upper-Air Sounding

Thermodynamic diagrams are graphical diagrams that are used to study the various thermodynamic processes occurring in the atmosphere. It is a tool by which the energy transformation that occurs during different thermodynamic processes can be studied. In such diagrams, various processes to which an air parcel can be subjected, like isobaric, isothermal, dry adiabatic, pseudo adiabatic, etc., can be represented in terms of isolines. The study further analyzes the vertical profile over the accident site using the model output. Given Figure 23 (a-f), which provides the atmospheric conditions during different time intervals. The upper air sounding generated by WRF also recorded that the atmosphere over the region was significantly adverse during the crash time. The wind profile shows a 25-knot wind blowing at 3 km (700 hPa) from sea level. The temperature profile is below freezing at 700 hPa.

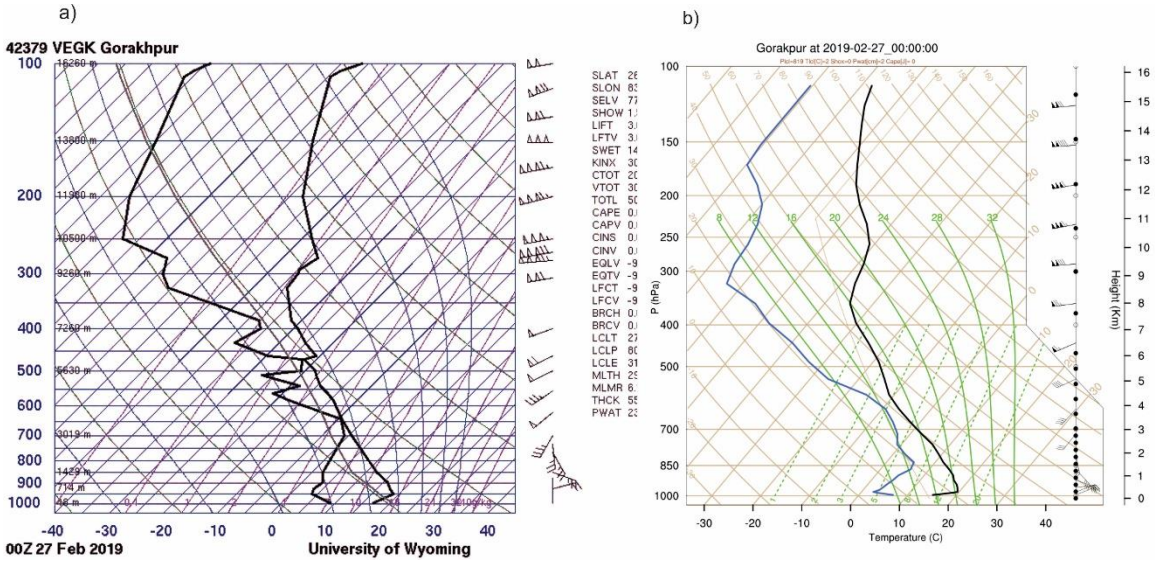

Figure 22: Skew-T diagram of the vertical atmosphere at (a) Gorakhpur Station, India at 5:45 LST (b) WRF model on 27 February 2019 at same location

For the vertical profile of the atmosphere, the upper air sounding data of Gorakhpur station is used (Figure 22a) at 5:45 LST. Both the model output Skew-T diagram and Gorakhpur station have recorded null CAPE values. This implies during this time no thunderstorm activity occurred over the accident regions. Vertical profile of dew point temperature also has the same behavior on both Figure 22 (a - b)

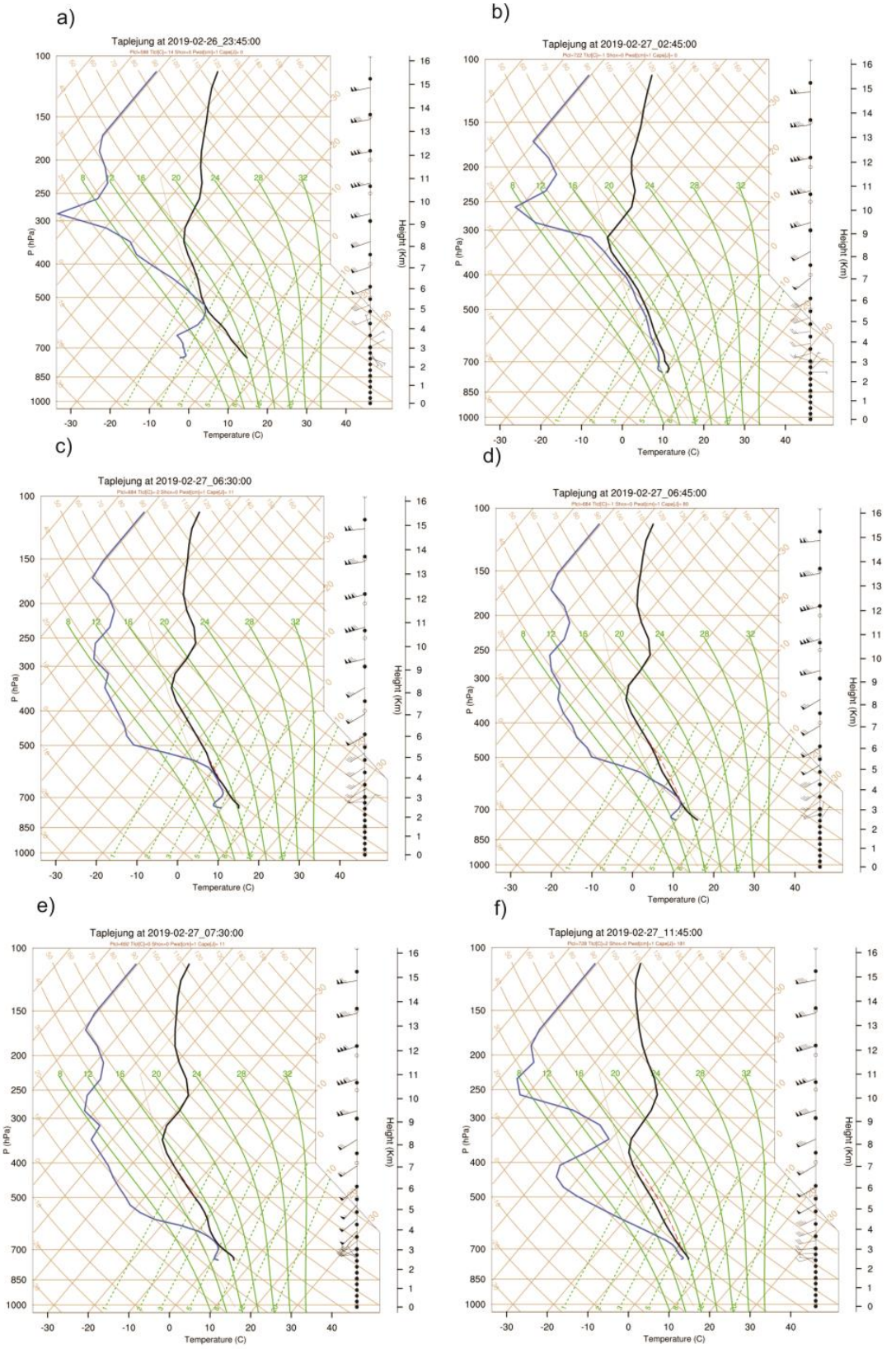

Figure 23: WRF model Skew-T diagram near Pathivara Peak i.e over the Eastern Nepal for the following times (a) 5:45LST (b) 8:30 LST (c) 12:30 LST (d) 12:45 LST (e) 1:15 LST (d) 17:45 LST

4.4 Discussion

This study raised multiple questions about the aviation weather hazards over the complex terrain. The different horizontal and vertical meteorological parametric analyses and their significant changes during the time of the accident Therefore, this study aims to answer whether the WRF model can simulate aviation weather over a complex topographical region or not, and what is the reason behind such helicopter flight crashes? Among several available global-to-regional models, we have selected the widely used WRF model for this study because it can simulate and is also used for route forecasts over the globe.

The different resolutions (9km, 3km, and 1km) represent the system's driving mechanism during the crash event and also capture the weather associated with it. The finest domain (D_3) contains four precipitation stations (Figure 7), and all stations recorded moderate rainfall over the 24 hours. The WRF model also captures as much as observed precipitation as shown in Figure 8. This illustrates that using a microphysics scheme that is suitable to perform better results over Nepal, especially for the aviation route forecast.

From the figures of infrared satellite images of INSAT-3D, we observed cloud mass over Nepal during the event. The event occurred during the winter season as the weather over Nepal was highly impacted by western disturbances (W.D). As moisture is contained, wind blows from the Mediterranean Sea, Caspian Sea, and the Black Sea approaches North-West India, especially the northern part of India at 30^0 N, by moving across Iraq, Iran, Afghanistan, Pakistan, and Nepal. The sea level pressure of the bigger domain (D_1) (Figure 10) illustrates that there are two or more closed isobars over the region. This means the weather over Nepal was influenced by W.D during the crash event.

The spatial and temporal distribution of radar reflectivity contours in the Figure 17 identifies the weather situation over Eastern Nepal in this case study. Regions with moderate to high reflectivity can be treated as restricted zones for Aircraft, whereas zones of intense reflectivity (< 40 dBZ) can be marked as prohibited areas. The reflectivity contours help route weather over the regions which is informative for the pilot.

The critical weather condition over the region further extends into microphysical processes. The weather conditions appear to inflight icing conditions. The saturated deep layer below freezing temperatures (Figure 18) can be seen together with the presence of significant amounts of cloud water (Figure 20 e-f) and graupel mixing ratios (Figure 20 c-d). All of these with a real-time picture of the accident site (Figure 13) low-level cloud ceiling, low amount of surface rainfall, and mixing ratios suggest that a quite favorable condition for the icing and severe loss in visibility was present along the flight path followed by aircraft at an altitude of 3.1 km AMSL.

In Figure 21 the entire Pathivara Peak has maximum relative humidity. A high percent of relative infers that the air was nearly saturated and sufficient enough for hydrometeors formation. A presence of fully saturated air mass at and below the freezing temperature level over the region and the temperature decreasing up to -19 ^{o}C at 500 hPa from 0 ^{o}C at 700 hPa (Figure 19) strongly suggest a highly favorable environment for the formation of supercooled water and graupel during the time of accident over the entire region.

The model doesn't forecast the sky as was said by DHM. However Figure 17 (b-c) shows there was presence of clouds and fog around the terrain and also Figure 18 (b-c), temperature below freezing points, the high concentration of droplets has high condensing and this condensation can causing icing on the rotors of the helicopter. In Figure 20 (e -f), the cloud mixing ratio shows the water content in clouds only at the top and upper elevation. As according to eyewitness and real time picture (Figure 13) before the crash time weather around the regions is gusty, light to moderate snowfall, this highlights either the clouds microphysics at local scale or the model failure because of coarse resolution.

CHAPTER-V

CONCLUSION AND RECOMMENDATION

5.1 Conclusion

To understand the regional aviation meteorological condition associated with the most recent fatal aircraft crash of 27 February 2019 in the complex terrain of Eastern Nepal Himalaya, the weather condition over the region has numerically been simulated using the WRF modeling system.

The prevailing weather conditions at the time of the accident, such as low ceiling with cloud base, light to moderate snowfall, poor visibility, below freezing temperatures, and high amounts of water droplets, suggest that the helicopter's rotor and windshield may have iced over.

The reflectivity value was more than 30 dBZ during the time of the accident based on the WRF model simulation. The atmosphere around the regions during the time of the accident was unfavorable based on the value of reflectivity. This implies moderate snowfall occurred during the accident time at 12:30 LST.

Icing could be major factor responsible for the fatal crash.

This research can provide the technique for a route forecast over the complex geographical regions of Nepal.

5.2 Recommendations

- Weather information plays a vital role in the aviation sector. WRF-ARW forecasts can be customized to generate and disseminate useful information about the meteorological condition to the pilots in advance for enhancing aviation safety.
- This research recommended that aviation stakeholders and pilots fly only after a clear route forecast over the complex geographical regions for the safety of flights.
- Multi-functioning aircraft flying system, and weather cameras, AWS should be installed in the airport to identify the real-time weather information.

5.3 Limitations

- The lack of proper hourly real-time meteorological observation data over the accident site prevented us from capturing arduous validations of model predictions.
- In the running WRF model, the default terrain resolution was used, which provides a little bit of a lack of terrain over the entire region. To minimize such topographic influence, lower resolution terrain data was used.

References

ARWUsersGuide.pdf. (n.d.). Retrieved June 12, 2022, from http://homepages.see.leeds.ac.uk/~lecrrb/wrf/aRWUsersGuide.pdf

Ashenden, R., & Marwitz, J. D. (1997). Turboprop Aircraft Performance Response to Various Environmental Conditions. *Journal of Aircraft*, *34*(3), 278–287. https://doi.org/10.2514/2.2196

Avolio, E., & Federico, S. (2018). WRF simulations for a heavy rainfall event in southern Italy: Verification and sensitivity tests. *Atmospheric Research*, *209*, 14–35. https://doi.org/10.1016/j.atmosres.2018.03.009

Cardoso, R. M., Soares, P. M. M., Miranda, P. M. A., & Belo-Pereira, M. (2013). WRF high resolution simulation of Iberian mean and extreme precipitation climate: WRF HIGH RESOLUTION SIMULATION OF IBERIAN PRECIPITATION. *International Journal of Climatology*, *33*(11), 2591–2608. https://doi.org/10.1002/joc.3616

Cassola, F., Ferrari, F., & Mazzino, A. (2015). Numerical simulations of Mediterranean heavy precipitation events with the WRF model: A verification exercise using different approaches. *Atmospheric Research*, *164–165*, 210–225. https://doi.org/10.1016/j.atmosres.2015.05.010

Chandra, A., Ghosh, S., Doshi, N., Deshpande, S., & Gumber, S. (2020). A Case Study on Assessing Cumulonimbus Induced Flight Vulnerabilities Over the Nepalese Himalayan Terrain. *Pure and Applied Geophysics*, *177*(10), 5041–5066. https://doi.org/10.1007/s00024-020-02541-w

Chawla, I., Osuri, K. K., Mujumdar, P. P., & Niyogi, D. (2018). Assessment of the Weather Research and Forecasting (WRF) model for simulation of extreme rainfall events in the upper Ganga Basin. *Hydrology and Earth System Sciences*, *22*(2), 1095–1117. https://doi.org/10.5194/hess-22-1095-2018

Chen, F., & Dudhia, J. (2001). Coupling an Advanced Land Surface–Hydrology Model with the Penn State–NCAR MM5 Modeling System. Part I: Model Implementation and Sensitivity. *Monthly Weather Review*, *129*(4), 569–585. https://doi.org/10.1175/1520-0493(2001)129<0569:CAALSH>2.0.CO;2

Chen, H., Gao, J., Wang, Y., Chen, Y., Sun, T., Carlin, J., & Zheng, Y. (2021). Radar reflectivity data assimilation method based on background-dependent hydrometeor retrieval: Comparison with direct assimilation for real cases. *Quarterly Journal of the Royal Meteorological Society*, *147*(737), 2409–2428. https://doi.org/10.1002/qj.4031

Chevuturi, A., Dimri, A. P., Das, S., Kumar, A., & Niyogi, D. (2015). Numerical simulation of an intense precipitation event over Rudraprayag in the central Himalayas during 13–14 September 2012. *Journal of Earth System Science*, *124*(7), 1545–1561. https://doi.org/10.1007/s12040-015-0622-5

Collier, E., & Immerzeel, W. W. (2015). High-resolution modeling of atmospheric dynamics in the Nepalese Himalaya. *Journal of Geophysical Research: Atmospheres*, *120*(19), 9882–9896. https://doi.org/10.1002/2015JD023266

Das, M. K., Islam, A. S., Karmakar, S., Khan, M. J. U., Mohammed, K., Islam, G. T., Bala, S. K., & Hopson, T. M. (2019). Synoptic flow patterns and large-scale characteristics of flash flood-producing rainstorms over northeast Bangladesh. *Meteorology and Atmospheric Physics*, 1–17.

Dasari, H. P., & Salgado, R. (2015). Numerical modelling of heavy rainfall event over Madeira Island in Portugal: Sensitivity to different micro physical processes. *Meteorological Applications*, *22*(1), 113–127. https://doi.org/10.1002/met.1375

Dudhia, J. (1989). Numerical Study of Convection Observed during the Winter Monsoon Experiment Using a Mesoscale Two-Dimensional Model. *Journal of the Atmospheric Sciences*, *46*(20), 3077–3107. https://doi.org/10.1175/1520-0469(1989)046<3077:NSOCOD>2.0.CO;2

El Afandi, G., Morsy, M., & El Hussieny, F. (2013). Heavy Rainfall Simulation over Sinai Peninsula Using the Weather Research and Forecasting Model. *International Journal of Atmospheric Sciences*, *2013*, 1–11. https://doi.org/10.1155/2013/241050

Gelpi, I. R., Gaztelumendi, S., Carreño, S., Hernández, R., & Egaña, J. (2016). *Study of NWP parameterizations on extreme precipitation events over Basque Country*.

Holton, J. R. (1973). An Introduction to Dynamic Meteorology. *American Journal of Physics*, *41*(5), 752–754. https://doi.org/10.1119/1.1987371

Insat-3d-brochure.pdf. (n.d.). Retrieved June 12, 2022, from https://www.isro.gov.in/sites/default/files/article-files/node/7954/insat-3d-brochure.pdf

Janić, Z. I. (2001). *Nonsingular implementation of the Mellor-Yamada level 2.5 scheme in the NCEP Meso model*. https://repository.library.noaa.gov/view/noaa/11409

Jarvis, C. H., & Stuart, N. (2001). A Comparison among Strategies for Interpolating Maximum and Minimum Daily Air Temperatures. Part II: The Interaction between Number of Guiding Variables and the Type of Interpolation Method. *Journal of Applied Meteorology*, *40*(6), 1075–1084. https://doi.org/10.1175/1520-0450(2001)040<1075:ACASFI>2.0.CO;2

Jee, J.-B., & Kim, S. (2017). Sensitivity Study on High-Resolution WRF Precipitation Forecast for a Heavy Rainfall Event. *Atmosphere*, *8*(6), 96. https://doi.org/10.3390/atmos8060096

Jiménez, P. A., Dudhia, J., González-Rouco, J. F., Montávez, J. P., García-Bustamante, E., Navarro, J., Vilà-Guerau de Arellano, J., & Muñoz-Roldán, A. (2013). An evaluation of WRF's ability to reproduce the surface wind over complex terrain based on typical circulation patterns: SURFACE WIND SIMULATION OVER COMPLEX TERRAIN. *Journal of Geophysical Research: Atmospheres*, *118*(14), 7651–7669. https://doi.org/10.1002/jgrd.50585

Kar, S. C., & Tiwari, S. (2016). Model simulations of heavy precipitation in Kashmir, India, in September 2014. *Natural Hazards: Journal of the International Society for the Prevention and Mitigation of Natural Hazards*, *81*(1), 167–188.

Karki, R., Hasson, S. ul, Gerlitz, L., Scholten, T., Schickhoff, U., & Böhner, J. (2017). Quantifying the added value of convection-permitting climate simulations in complex terrain: A systematic evaluation of WRF over the Himalayas. *Earth System Dynamics*, *8*, 507–528. https://doi.org/10.5194/esd-8-507-2017

Karki, R., Hasson, S. ul, Gerlitz, L., Talchabhadel, R., Schenk, E., Schickhoff, U., Scholten, T., & Böhner, J. (2018). WRF-based simulation of an extreme precipitation event over the Central Himalayas: Atmospheric mechanisms and their representation by microphysics parameterization schemes. *Atmospheric Research*, *214*, 21–35. https://doi.org/10.1016/j.atmosres.2018.07.016

Kim, J.-H., & Chun, H.-Y. (2012). A Numerical Simulation of Convectively Induced Turbulence above Deep Convection. *Journal of Applied Meteorology and Climatology*, *51*(6), 1180–1200. https://doi.org/10.1175/JAMC-D-11-0140.1

Kumar, M. S., Shekhar, M. S., Krishna, S. R., Bhutiyani, M. R., & Ganju, A. (2012). Numerical simulation of cloud burst event on August 05, 2010, over Leh using WRF mesoscale model. *Natural Hazards*, *62*(3), 1261–1271.

Kumar, P., Bhattacharya, B. K., & Pal, P. K. (2015). Evaluation of Weather Research and Forecasting Model Predictions Using Micrometeorological Tower Observations. *Boundary-Layer Meteorology*, *157*(2), 293–308. https://doi.org/10.1007/s10546-015-0061-5

Kumar, V. V., Jakob, C., Protat, A., May, P. T., & Davies, L. (2013). The four cumulus cloud modes and their progression during rainfall events: A C-band polarimetric radar perspective: TROPICAL CUMULUS CLOUDS. *Journal of Geophysical Research: Atmospheres*, *118*(15), 8375–8389. https://doi.org/10.1002/jgrd.50640

Lee, J., Shin, H. H., Hong, S.-Y., Jiménez, P. A., Dudhia, J., & Hong, J. (2015). Impacts of subgrid-scale orography parameterization on simulated surface layer wind and monsoonal precipitation in the high-resolution WRF model: Impact of orography scheme on rainfall. *Journal of Geophysical Research: Atmospheres*, *120*(2), 644–653. https://doi.org/10.1002/2014JD022747

LeMone, M. A., & Zipser, E. J. (1980). Cumulonimbus Vertical Velocity Events in GATE. Part I: Diameter, Intensity and Mass Flux. *Journal of the Atmospheric Sciences*, *37*(11), 2444–2457. https://doi.org/10.1175/1520-0469(1980)037<2444:CVVEIG>2.0.CO;2

MAHBUB ALAM, M. (2014). Impact of cloud microphysics and cumulus parameterization on simulation of heavy rainfall event during 7–9 October 2007 over Bangladesh. *Journal of Earth System Science*, *123*(2), 259–279. https://doi.org/10.1007/s12040-013-0401-0

Marwitz, J. (2013). Comments on "Characterization of Aircraft Icing Environments with Supercooled Large Drops for Application to Commercial Aircraft Certification." *Journal of Applied Meteorology and Climatology*, *52*(7), 1670–1672. https://doi.org/10.1175/JAMC-D-12-096.1

Matsuda, K., & Onishi, R. (2019). Turbulent enhancement of radar reflectivity factor for polydisperse cloud droplets. *Atmospheric Chemistry and Physics*, *19*(3), 1785–1799. https://doi.org/10.5194/acp-19-1785-2019

Maussion, F., Scherer, D., Mölg, T., Collier, E., Curio, J., & Finkelnburg, R. (2014). Precipitation Seasonality and Variability over the Tibetan Plateau as Resolved by the High Asia Reanalysis*. *Journal of Climate*, *27*(5), 1910–1927. https://doi.org/10.1175/JCLI-D-13-00282.1

Medina, S., Houze, R. A., Kumar, A., & Niyogi, D. (2010). Summer monsoon convection in the Himalayan region: Terrain and land cover effects. *Quarterly Journal of the Royal Meteorological Society*, n/a-n/a. https://doi.org/10.1002/qj.601

Mlawer, E. J., Taubman, S. J., Brown, P. D., Iacono, M. J., & Clough, S. A. (1997). Radiative transfer for inhomogeneous atmospheres: RRTM, a validated correlated-k model for the longwave. *Journal of Geophysical Research: Atmospheres*, *102*(D14), 16663–16682. https://doi.org/10.1029/97JD00237

Moya-Álvarez, A. S., Gálvez, J., Holguín, A., Estevan, R., Kumar, S., Villalobos, E., Martínez-Castro, D., & Silva, Y. (2018). Extreme Rainfall Forecast with the WRF-ARW Model in the Central Andes of Peru. *Atmosphere*, *9*(9), 362. https://doi.org/10.3390/atmos9090362

Navale, A., Singh, C., Budakoti, S., & Singh, S. K. (2020). Evaluation of season long rainfall simulated by WRF over the NWH region: KF vs. MSKF. *Atmospheric Research*, *232*, 104682. https://doi.org/10.1016/j.atmosres.2019.104682

NCEP GDAS/FNL 0.25 Degree Global Tropospheric Analyses and Forecast Grids. (2020). https://cmr.earthdata.nasa.gov/search/concepts/C1214111016-SCIOPS

Norris, J., Carvalho, L. M. V., Jones, C., & Cannon, F. (2015). WRF simulations of two extreme snowfall events associated with contrasting extratropical cyclones over the western and central Himalaya. *Journal of Geophysical Research: Atmospheres*, *120*(8), 3114–3138. https://doi.org/10.1002/2014JD022592

Ntwali, D., Ongoma, V., & Ogwang, B. A. (2016). The Impacts of Topography on Spatial and Temporal Rainfall Distribution over Rwanda Based on WRF Model. *Atmospheric and Climate Sciences*, *6*(2), 720–726. https://doi.org/10.4236/acs.2016.62013

Orr, A., Listowski, C., Couttet, M., Collier, E., Immerzeel, W., Deb, P., & Bannister, D. (2017). Sensitivity of simulated summer monsoonal precipitation in Langtang Valley, Himalaya, to cloud microphysics schemes in WRF. *Journal of Geophysical Research: Atmospheres*, *122*(12), 6298–6318.

Rajeevan, M., Kesarkar, A., Thampi, S. B., Rao, T. N., Radhakrishna, B., & Rajasekhar, M. (2010). Sensitivity of WRF cloud microphysics to simulations of a severe thunderstorm event over Southeast India. *Annales Geophysicae*, *28*(2), 603–619. https://doi.org/10.5194/angeo-28-603-2010

Regmi, R. P. (2015a). Aviation Hazards Over the Jomsom Airport of Nepal as Revealed by Numerical Simulation of Local Flows. *Journal of Institute of Science and Technology*, *19*(1), 111–120. https://doi.org/10.3126/jist.v19i1.13836

Regmi, R. P. (2015b). Aviation Hazards in the Sky over Thada as Revealed by Meso-scale Meteorological Modeling. *Journal of Institute of Science and Technology*, *19*(2), 65–70. https://doi.org/10.3126/jist.v19i2.13854

Regmi, R. P., Kitada, T., & Kurata, G. (2003). Numerical Simulation of Late Wintertime Local Flows in Kathmandu Valley, Nepal: Implication for Air Pollution Transport. *Journal of Applied Meteorology and Climatology*, *42*(3), 389–403. https://doi.org/10.1175/1520-0450(2003)042<0389:NSOLWL>2.0.CO;2

Regmi, R. P., & Maharjan, S. (2015). Trapped mountain wave excitations over the Kathmandu valley, Nepal. *Asia-Pacific Journal of Atmospheric Sciences*, *51*(4), 303–309. https://doi.org/10.1007/s13143-015-0078-1

Sand, W. R., Cooper, W. A., Politovich, M. K., & Veal, D. L. (1984). Icing Conditions Encountered by a Research Aircraft. *Journal of Climate and Applied Meteorology*, *23*(10), 1427–1440. https://doi.org/10.1175/0733-3021-23.10.1427

Sauvageot, H., & Omar, J. (1987). Radar Reflectivity of Cumulus Clouds. *Journal of Atmospheric and Oceanic Technology*, *4*(2), 264–272. https://doi.org/10.1175/1520-0426(1987)004<0264:RROCC>2.0.CO;2

Sharman, R. D., Doyle, J. D., & Shapiro, M. A. (2012). An Investigation of a Commercial Aircraft Encounter with Severe Clear-Air Turbulence over Western Greenland. *Journal of Applied Meteorology and Climatology*, *51*(1), 42–53. https://doi.org/10.1175/JAMC-D-11-044.1

Shrestha, R. K., Connolly, P. J., & Gallagher, M. W. (2017). Sensitivity of WRF cloud microphysics to simulations of a convective storm over the Nepal Himalayas. *The Open Atmospheric Science Journal*, *11*(1).

Singh, K. S., Bonthu, S., Purvaja, R., Robin, R. S., Kannan, B. A. M., & Ramesh, R. (2018). Prediction of heavy rainfall over Chennai Metropolitan City, Tamil Nadu, India: Impact of microphysical parameterization schemes. *Atmospheric Research*, *202*, 219–234.

Skamarock, W. C., Klemp, J. B., Dudhia, J., Gill, D. O., Liu, Z., Berner, J., Wang, W., Powers, J. G., Duda, M. G., Barker, D. M., & Huang, X.-Y. (n.d.). *A Description of the Advanced Research WRF Model Version 4*. 162.

Tanessong, R. S., Vondou, D. A., Djomou, Z. Y., & Igri, P. M. (2017). WRF high resolution simulation of an extreme rainfall event over Douala (Cameroon): A case study. *Modeling Earth Systems and Environment*, *3*(3), 927–942. https://doi.org/10.1007/s40808-017-0343-7

Thompson, G., Rasmussen, R. M., & Manning, K. (2004). Explicit Forecasts of Winter Precipitation Using an Improved Bulk Microphysics Scheme. Part I: Description and Sensitivity Analysis. *Monthly Weather Review*, *132*(2), 519–542. https://doi.org/10.1175/1520-0493(2004)132<0519:EFOWPU>2.0.CO;2

Whiteman, C. D. (2000). *Mountain Meteorology: Fundamentals and Applications*. Oxford University Press.

Zeyaeyan, S., Fattahi, E., Ranjbar, A., Azadi, M., & Vazifedoust, M. (2017). Evaluating the Effect of Physics Schemes in WRF Simulations of Summer Rainfall in North West Iran. *Climate, 5*(3), 48. https://doi.org/10.3390/cli5030048

Appendix

Appendix I: Synoptic data at Taplejung station (1= Surface Pressure, 2= Sea Level Pressure, 3= Relative Humidity, 4= Air Temperature, 5= Dew Point Temperature, 6= Visibility, 7= Wind Speed)

S.N	Date	0 UTC	3 UTC	6 UTC	9 UTC	12 UTC
1	25-Feb-2019	825.1	825.7	825.1	822.2	823.1
2		1009.2	1009.1	1008.5	1007	1006.5
3		93	85	58	55	67
4		10.2	11.8	15	16.8	12.6
5		8.8	9.6	6.8	7.9	6.6
6		6	6	6	3	3
7		0	0	4	10	4
1	26-Feb-2019	823.7	825.4	826.7	823.7	822.5
2		1005.6	1010.9	1012.2	1009.2	1005.7
3		85	64	69	62	68
4		6.4	9.8	15.4	17.2	13.2
5		3.6	3.6	10.4	9.8	7.2
6		6	8	6	6	5
7		0	0	0	4	10
1	27-Feb-2019	823.1	825.9	826.3	824.2	822.5
2		1006.3	1009.1	1009.5	1007.4	1003
3		74	75	78	78	91
4		7.2	8.4	9	9.2	8
5		2.2	3.8	5.5	5.5	6
6		6	5	5	3	3
7		0	0	0	0	0
1	28-Feb-2019	823	825.4	825	823	821.6
2		1009	1013.7	1013.3	1011.3	1007.6
3		96	92	81	74	76
4		5.8	7.2	4.8	11.6	8.6
5		5	4.7	2	7.5	5
6		6	3	4	5	6
7		0	0	0	0	2

Appendix II: a) Areal view of crash site b) Rescue operation of 9N- AMI c) Air Dynasty Helicopter (Source: Helicopter accident investigation commission, 2020)

a)

b)

c)